



**MATHEMATICAL MODELLING OF LOG NORMAL ATMOSPHERIC
TURBULENCE CHANNELS**

SERKAN GÖRSE

JUNE 2018

**MATHEMATICAL MODELLING OF LOG NORMAL ATMOSPHERIC
TURBULENCE CHANNELS**

**A THESIS SUBMITTED TO
THE GRADUATE SCHOOL OF NATURAL AND APPLIED
SCIENCES OF
ÇANKAYA UNIVERSITY**



**BY
SERKAN GÖRSE**

**IN PARTIAL FULFILLMENT OF THE REQUIREMENTS FOR THE
DEGREE OF
MASTER OF SCIENCE
IN
THE DEPARTMENT OF
ELECTRONIC AND COMMUNICATION ENGINEERING**

JUNE 2018

**Title of the Thesis: Mathematical Modelling of Log Normal Atmospheric
Turbulence Channels**

Submitted by Serkan GÖRSE

Approval of the Graduate School of Natural and Applied Sciences, Cankaya
University.


Prof. Dr. Can ÇOGUN
Director

I certify that this thesis satisfies all the requirements as a thesis for the degree of
Master of Science.


Dr. Özgür ERGÜL
Head of Department

This is to certify that we have read this thesis and that in our opinion it is fully
adequate, in scope and quality, as a thesis for the degree of Master of Science.


Assoc. Prof. Dr. Orhan GAZİ
Supervisor

Examination Date: 17.07.2018

Examining Committee Members

Prof. Dr. Yahya Kemal BAYKAL

(Cankaya Univ.)



Assoc. Prof. Dr. Orhan GAZİ

(Cankaya Univ.)



Assist. Prof. Dr. Javad RAHEBİ

(THK Univ.)



STATEMENT OF NON-PLAGIARISM PAGE

I hereby declare that all information in this document has been obtained and presented in accordance with academic rules and ethical conduct. I also declare that, as required by these rules and conduct, I have fully cited and referenced all material and results that are not original to this work.

Name, Last Name : Serkan
GÖRSE

Signature :

Date : 17.07.2018

ABSTRACT

Mathematical Modeling of Log Normal Turbulence Channels

GÖRSE, Serkan

M.Sc., Department of Electronic and Communication Engineering

Supervisor: Assoc. Prof. Dr. Orhan GAZI

July 2018, 68 pages

In this thesis work we demonstrated the development of a mathematical model for those systems involving complex numerical integration formulas. For this purpose, we considered two-hop communication systems. For the two-hop communication systems, the end-to-end performance depends on the harmonic mean of hop SNRs. For log-normal distributed channels, we considered two-hop communication systems and calculated the harmonic mean of two SNRs. The calculated harmonic mean value is in integral form and it need to be calculated numerically. We showed that such an integral formula can be expressed approximately using simple mathematical expressions. For this purpose, we used curve fitting utility of the MATLAB platform and approximated the harmonic mean expression by a Gaussian like distribution. Using the approximation formula, cumulative distribution function, moments generating function, moments, outage probability, amount of fading and transmission error probability are calculated in closed forms. The proposed approach presented in this thesis work can be used for the systems having long and complex performance calculation formulas.

Keywords: Performance of Free Space Optic, Harmonic Mean, Performance Analyses, Probability Density Function.

ÖZ

Log Normal Türbülans Kanallarının Matematiksel Modellemesi

GÖRSE, Serkan

Yüksek Lisans, Elektronik ve Haberleşme Mühendisliği Anabilim Dalı

Tez Yöneticisi: Assoc. Prof. Dr. Orhan GAZİ

Temmuz 2018, 68 sayfa

Bu tez çalışmasında karmaşık numerik hesap gerektiren matematiksel bir denklemin daha basit ve kapalı formda olan matematiksel bir ifade ile yaklaşık olarak elde edilmesine yönelik bir çalışma sunulmaktadır. Bunun için iki atlamalı haberleşme sistemleri düşünülmüştür. İki atlamalı haberleşme sistemlerinin uçtan-uca olan performansları atlamalardaki SNR değerlerinin harmonik ortalamasına bağlıdır. Çalışmamızda iki atlamalı ve Log-normal dağılımına sahip iletişim sistemlerinin atlama noktalarındaki SNR dağılımlarının harmonik ortalama değerini integral formunda hesapladık. Daha sonra hesaplamış olduğumuz integral formundaki karışık matematiksel ifadeyi MATLAB derleyicisinin curve-fitting aracını kullanarak daha basit matematiksel ifadelerle yaklaşık olarak hesapladık. Hesapladığımız yaklaşık değer formülü kapalı formdadır ve bu formülü kullanarak kümülatif dağılım fonksiyonu, moment üretim fonksiyonu, kesinti olasılığı fonksiyonu, gönderim hata olasılığı gibi fonksiyonları kapalı formda hesapladık. Son olarak da hesapladığımız fonksiyonları kullanarak sistemin performansını gönderim hata olasılığı grafiği ile göstermiş olduk.

Anahtar Kelimeler: Serbest Uzay Optik Sistem Performansı, Harmonik Ortalama, Performans analizi, Olası yoğunluk fonksiyonu.

ACKNOWLEDGEMENTS

The author wishes to express his deepest gratitude to his supervisor Assoc. Prof. Dr. Orhan GAZİ for his supervision, special guidance, suggestions, and encouragement through the development of this thesis.

The author would also like to thank Prof. Dr. Yahya Kemal BAYKAL for his suggestions and comments during the study.

It is a pleasure to express my special thanks to my family for their strong support.

TABLE OF CONTENTS

STATEMENT OF NON- PLAGIARISM.....	I
ABSTRACT.....	ii
ÖZ.....	iii
ACKNOWLEDGEMENTS.....	iv
TABLE OF CONTENTS.....	v
LIST OF FIGURES.....	vii
LIST OF TABLES.....	ix
LIST OF ABBREVIATIONS.....	x
CHAPTERS:	
1. INTRODUCTION.....	1
1.1. Background.....	1
1.2. Objectives.....	2
1.3. Organization of Thesis.....	2
2. Mathematical Modeling of Log Normal Atmospheric Turbulence Channel.....	4
2.1. Probability Density Function of Log Normal Distribution.....	4
2.2. Joint Probability Density Function.....	6
2.3. Detection of Best Fitting Curves in MATLAB.....	8
2.4. Coefficient Analyze According to Distance.....	12
2.5. Coefficient Analyze According to Turbulence Strength.....	14
2.6. Comparison MATLAB Model and Integral Form of Probability Density Function.....	21
3. Calculations of Functions.....	22
3.1. Cumulative Distribution Function (CDF).....	22
3.2. Moment Generating Function (MGF).....	23
3.3. Moments.....	24

3.4.	Outage Probability	24
3.5.	Amount of Fading.....	25
3.6.	Probability of Transmission Error Rate.....	28
3.7.	Average Probability of Transmission Error Rate.....	46
4.	CONCLUSION.....	48
	REFERENCES.....	50
	APPENDICES.....	53
	A. CURRICULUM VITAE.....	53



LIST OF FIGURES

FIGURES

Figure 1	Probability Density Function to Signal Noise Ratio.....	8
Figure 2	Gaussian Equation Model	9
Figure 3	Polynomial Equation Model.....	10
Figure 4	Fourier Equation Model	11
Figure 5	Change of A with respect to L.....	13
Figure 6	Change of B with respect to L.....	13
Figure 7	Change of C with respect to L.....	14
Figure 8	Change of A with respect to Cn^2	15
Figure 9	Change of B with respect to Cn^2	15
Figure 10	Change of C with respect to Cn^2	16
Figure 11	Polynomial Equation Constant Values to Cn^2 Graphs.....	20
Figure 12	Comparison of Result.....	21
Figure 13	Change of A with respect to L for $\bar{\mu} = 5$	29
Figure 14	Change of B with respect to L for $\bar{\mu} = 5$	30
Figure 15	Change of C with respect to L for $\bar{\mu} = 5$	30
Figure 16	Comparisons of Results for $\bar{\mu} = 5$	31
Figure 17	Change of A with respect to L for $\bar{\mu} = 10$	32
Figure 18	Change of B with respect to L for $\bar{\mu} = 10$	32
Figure 19	Change of C with respect to L for $\bar{\mu} = 10$	33
Figure 20	Comparisons of Results for $\bar{\mu} = 10$	33
Figure 21	Change of A with respect to L for $\bar{\mu} = 15$	34
Figure 22	Change of B with respect to L for $\bar{\mu} = 15$	34
Figure 23	Change of C with respect to L for $\bar{\mu} = 15$	35
Figure 24	Comparisons of Results for $\bar{\mu} = 15$	35
Figure 25	Change of A with respect to L for $\bar{\mu} = 20$	36

Figure 26	Change of B with respect to L for $\bar{\mu} = 20$	36
Figure 27	Change of C with respect to L for $\bar{\mu} = 20$	37
Figure 28	Comparisons of Results for $\bar{\mu} = 20$	37
Figure 29	Change of A with respect to L for $\bar{\mu} = 25$	38
Figure 30	Change of B with respect to L for $\bar{\mu} = 25$	38
Figure 31	Change of C with respect to L for $\bar{\mu} = 25$	39
Figure 32	Comparisons of Results for $\bar{\mu} = 25$	39
Figure 33	Change of A with respect to L for $\bar{\mu} = 30$	40
Figure 34	Change of B with respect to L for $\bar{\mu} = 30$	40
Figure 35	Change of C with respect to L for $\bar{\mu} = 30$	41
Figure 36	Comparisons of Results for $\bar{\mu} = 30$	41
Figure 37	Change of A with respect to L for $\bar{\mu} = 35$	42
Figure 38	Change of B with respect to L for $\bar{\mu} = 35$	42
Figure 39	Change of C with respect to L for $\bar{\mu} = 35$	43
Figure 40	Comparisons of Results for $\bar{\mu} = 35$	43
Figure 41	Change of A with respect to L for $\bar{\mu} = 40$	44
Figure 42	Change of B with respect to L for $\bar{\mu} = 40$	44
Figure 43	Change of C with respect to L for $\bar{\mu} = 40$	45
Figure 44	Comparisons of Results for $\bar{\mu} = 40$	45
Figure 45	Average Bit Error Rate to SNR.....	47

LIST OF TABLES

TABLES

Table 1	Constant Values for 50 Pieces of Cn^2	17
Table 2	Constant Values for 50 Pieces of Cn^2	18
Table 3	List of Coefficients for Different $\bar{\mu}$ Values.....	46



LIST OF ABBREVIATIONS

FSO	Free Space Optics
PDF	Probability Density Function
SNR	Signal Noise Ratio
CDF	Cumulative Density Function
MGF	Moment Generating Function
BER	Bit Error Rate

CHAPTER 1

INTRODUCTION

1.1 Background

In today's conditions, the need for more favorable opportunities, environment and tools in the communication world have increased. Every passing day, the necessity of optic communication systems is escalating in various areas such as telephone, networks data transmission, integrated optic mechanisms, cable television systems, transportation, military and medical applications in the direction of the above-mentioned requirements. High speed data transmission speed for the optical networks is possible.

In present technology, the optical communication systems are more preferred than the other communication systems. Optical communication systems have some advantages over the classical communication systems, the existence of the silicium which is the raw material of the optical wave guide as a glut in the nature, stoutness of the isolation, the velocity head, stableness, being not affected by the electromagnetic effects, reliability, cost-efficiency and specifically having a large capacity and low transmission loss with high band width. The use of the optical fibers which are the dielectric transmission medium is increasing alongside the wired communication media such as the copper cable and coaxial cable. Because it has much less loss than the free space wireless communication. Its sufficiency to work in coordination with the old communication systems is one of the significant characteristic of optical fibers.

Free Space Optic (FSO) systems transmit data for telecommunications or computer networks. In contrast to the radio frequency networks, free space optical (FSO) communications provide many advantages which cause FSO to become increasingly popular and studied over the past decade. Most important advantages of FSO

communication systems are transmission rate, low cost, systematical, portability security and licensing. Free space optical systems use light propagation in free space. Free space means air, outer space or something similar. Today we use fiber optic cables for computer networks or high speed communication. Fiber optic cables cannot be useful when the physical connection is not possible. Systems which include fiber optic cables have high level cost in some places. For example, fiber deployment in urban areas could cost \$300000-\$700000 per kilometer without other installation cost. A FSO system with same transmission rate could be more economic at a price of \$18000 [4,5]. Although FSO systems can be a good solution to overcome these disadvantages, there are limitations as well. The degrading factors for optical communication include the fact that rain, dust, snow, fog or smog can obstruct the transmission path and these factors can shut down the network. Scientists try to improve FSO systems to avoid the air conditions that lead to limitations on communication systems. They develop many hardware and communication technique to overcome these difficulties.

1.2 Objectives

The main aim of this thesis is to develop a mathematical model for free space optic communication systems over log normal turbulence channels. There are many factors that affect the optical communication's system performance on atmosphere. Distance, temperature, altitude and pressure are some of important factors. Performance of FSO systems are analyzed by changing distance. These effects are demonstrated by graphs which are plotted by MATLAB in details. Cumulative density function, moments generating function, amount of fading and bit error rate are calculated.

1.3 Organization of the Thesis

This thesis is divided into four chapters. All analyses are studied to calculate performance of FSO channels over log normal turbulence channels. Results are compared with different distance and turbulence strength.

Chapter-1 covers an introduction and a background for free space optic's communication systems and portrays objectives of this thesis.

Chapter-2 involves the mathematical modeling of optic communication channels over log normal atmospheric turbulence channels.

Chapter-3 explains calculation of cumulative density function, moment generation function, moments, amount of fading and bit error rate with the mathematical model developed in Chapter-2.

Chapter-4 is the conclusion part.



CHAPTER 2

MATHEMATICAL MODELLING OF LOG NORMAL ATMOSPHERIC TURBULANCE CHANNELS

2.1 Probability Density Function of Log Normal Distribution

In this part of thesis, we work on the performance of FSO channels by investigating their outage probability and the average capacity, respectively. Thus, we derive closed form expressions for the outage probability and the average capacity of optical links over atmospheric turbulence induced fading channels modeled by the log normal turbulence distribution with respect to the turbulence strength, as well as the influence of other important system's parameters, such as optical link length and the receiver's aperture diameter.

Firstly, we calculate the probability density function by utilizing the harmonic mean of two signals. Given two numbers X_1 and X_2 , the harmonic means of X_1 and X_2 , is defined as [6, 9]

$$\mu_H (X_1, X_2) = \frac{2X_1X_2}{X_1 + X_2} \quad (2.1)$$

We define three parameters (x z w) to express this equation more easily. These parameters are equal to

$$w = X_1 + X_2 \quad z = 2X_1X_2 \quad x = \frac{z}{w}. \quad (2.2)$$

For the harmonic mean calculation of two random variables, we consider the random variables having log-normal distribution. The probability density function equation of the log normal turbulence as given by

$$p(x) = \frac{1}{2\mu\sigma\sqrt{2\pi}} \exp\left(-\frac{\left(\ln\left(\frac{\mu}{x}\right) + \sigma^2\right)^2}{8\sigma^2}\right) \quad (2.3)$$

where σ is the standard deviation of the log normal distribution, which depends on the channel's characteristics and it is calculated as [9, 17]

$$\sigma^2 = \exp\left[\frac{0.49\delta^2}{\left(1 + 0.18d^2 + 0.56\delta^{\frac{12}{5}}\right)^{\frac{7}{6}}} + \frac{0.51\delta^2}{\left(1 + 0.9d^2 + 0.62d^2\delta^{\left(\frac{12}{5}\right)}\right)^{\frac{5}{6}}}\right] - 1 \quad (2.4)$$

where

$$d = \sqrt{\frac{kD^2}{4L}}$$

and

$$k = \frac{2\pi}{\lambda}$$

is the optical wave number, L is the length of the optical link and D is the receiver's aperture diameter. The parameter δ is called Rytov variance and it is defined as

$$\delta^2 = 1.23 C_n^2 k^{\frac{7}{6}} L^{\frac{11}{6}}. \quad (2.5)$$

where C_n^2 is the altitude which is dependent on the turbulence strength varying from 10^{-17} to $10^{-13} m^{-2/3}$ according to atmospheric turbulence conditions [2,8]. The instantaneous electrical signal to noise ratio (SNR) is given as

$$\mu = \left(\frac{\eta I^2}{N_0}\right) = \frac{s^2}{N_0}$$

and the average electrical SNR is calculated as

$$\bar{\mu} = \eta \frac{E[I]}{N_0}.$$

Now we must use error function to define *pdf* equation of log normal model more simply.

The exponential term in log-normal distribution in (2.3) can be expressed as in

$$p(x) = \exp\left(-\frac{(\ln(\frac{\mu}{x}) + \sigma^2)^2}{8\sigma^2}\right) \rightarrow \exp\left[-\left(\frac{1}{8\sigma^2}\right) \left[\ln\left(\frac{\mu}{x}\right)\right]^2 + \sigma^4 + 2\sigma^2 \ln\left(\frac{\mu}{x}\right)\right]. \quad (2.6)$$

After this operation, probability density functions of log normal distribution take the form

$$p(x) = \frac{1}{2\sigma\sqrt{2\pi}} \exp\left[-\frac{\sigma^2}{8}\right] \bar{\mu}^{-\left(\frac{1}{4}\right)} \mu^{\frac{1}{4}} \exp\left[-\left(\frac{1}{8\sigma^2}\right) \left[\ln\left(\frac{\mu}{x}\right)\right]^2\right]. \quad (2.7)$$

If we define the constant value K as in

$$K = \frac{1}{2\sigma\sqrt{2\pi}} \exp\left[-\frac{\sigma^2}{8}\right] \bar{\mu}^{-\left(\frac{1}{4}\right)} \quad (2.8)$$

then the log-normal distribution in (2.7) can be written as in (2.9)

At the end of these steps pdf equation transformed to an easier form which is expressed as equation(2.9).

$$p(x) = K \cdot \mu^{\frac{1}{4}} \cdot \exp\left[\left[\ln\left(\frac{\mu}{x}\right)\right]^2\right] \quad (2.9)$$

2.2 Joint Probability Density Function

The joint pdf of the random variables Z, W , i.e., $P_{z,w}(z, w)$ can be derived using the Jacobian transformation. We can write the harmonic mean of X_1 and X_2 as $X = Z/W$ where $X = 2X_1X_2$ and $W = X_1 + X_2$. Using [12, Sec. 6.2], the PDF of X can be written as,

$$p_x(x) = \int_{-\infty}^{\infty} |w| P_{z,w}(xw, w) dw \quad (2.10)$$

which can be evaluated with the help of [7, Eq. (3.383.4)] yielding,

$$P_{z,w} = \frac{1}{2\Delta} [P_{x_1, x_2}(X_{11}, X_{21}), P_{x_1, x_2}(X_{12}, X_{22})] \quad (2.11)$$

in which we have

$$X_{11}, X_{21} = w \pm \frac{\sqrt{w^2 - 2z}}{2}, X_{12}, X_{22} = w \pm \frac{\sqrt{w^2 - 2z}}{2}, \Delta = \sqrt{w^2 - 2z} \quad (2.12)$$

Substituting the parameters in (2.11), and the log-normal distribution expression in (2.9) into we obtain (2.14).

$$P_{z,w}(z, w) = \frac{1}{2\sqrt{w^2 - 2z}} [P(x_{11})P(x_{21}) + P(x_{12})P(x_{22})] \quad (2.13)$$

$$P_{z,w}(z, w) = \frac{2}{2\sqrt{w^2 - 2z}} \left[\begin{array}{l} K \left(\frac{(w + \Delta)}{2} \right)^{\frac{1}{4}} \exp \left(\frac{1}{8\sigma^2} \left[\ln \left(\frac{(w + \Delta)}{2} \frac{1}{x} \right) \right]^2 \right) \\ K \left(\frac{(w - \Delta)}{2} \right)^{\frac{1}{4}} \exp \left(\frac{1}{8\sigma^2} \left[\ln \left(\frac{(w - \Delta)}{2} \frac{1}{x} \right) \right]^2 \right) \end{array} \right]. \quad (2.14)$$

The probability density function of $X = Z/W$ can be calculated using

$$P_X(x) = \int_{2x}^{\infty} w P_{z,w}(xw, w) dw$$

leading to

$$p(x) = K \int_{2x}^{\infty} w^{-\left(\frac{3}{4}\right)} (w - 2x)^{-\left(\frac{1}{2}\right)} \exp \left(-\frac{1}{8\sigma^2} \left[\left[\frac{w + \Delta}{2a} \right]^2 \left[\frac{w - \Delta}{2a} \right]^2 \right] \right) dw. \quad (2.15)$$

This integration is cannot be expressed in closed form. We write some code in MATLAB to calculate this integral and we plot its graph vs. SNR, i.e., vs. x . The graph of this $p(x)$ is shown on Fig. 1.

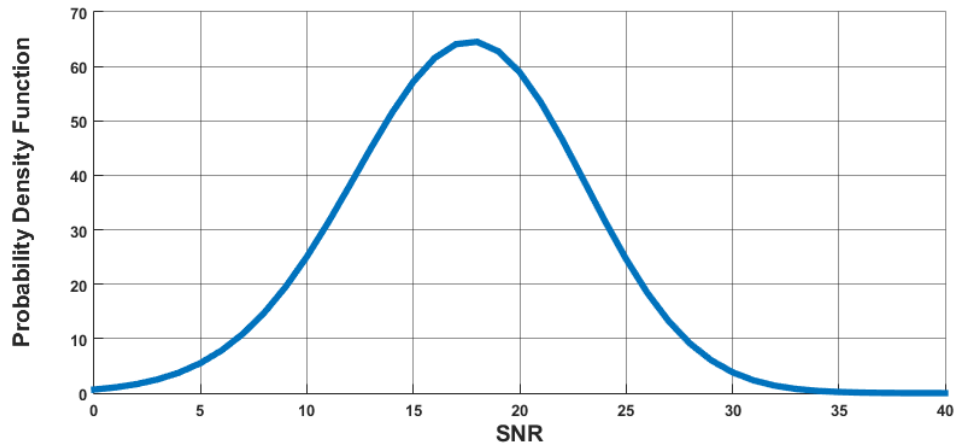


Figure 1 Probability Density Function to Signal Noise Ratio

2.3 Detection of Best Fitting Curves in MATLAB

MATLAB curve fitting option is used to find the best mathematical expression that approximates the probability density function in (2.15) closely. To express the integration defined in (2.15) in closed form, different curve fitting models of the MATLAB can be utilized. The typical curve fitting models available in MATLAB are Gaussian, Fourier, and Polynomial. We decide for Gaussian model with 1st degree. Because, we obtain best fitting performance and simple integration in Gaussian model. Performance analysis and coefficients values of Gaussian model are shown in Fig. 2, Fourier model is shown in Fig. 3 and Polynomial model is shown in Fig. 4. At the same time, we compare the number of terms, general mode of equation, goodness of fit and coefficient values in Fig. 2, 3 and 4.

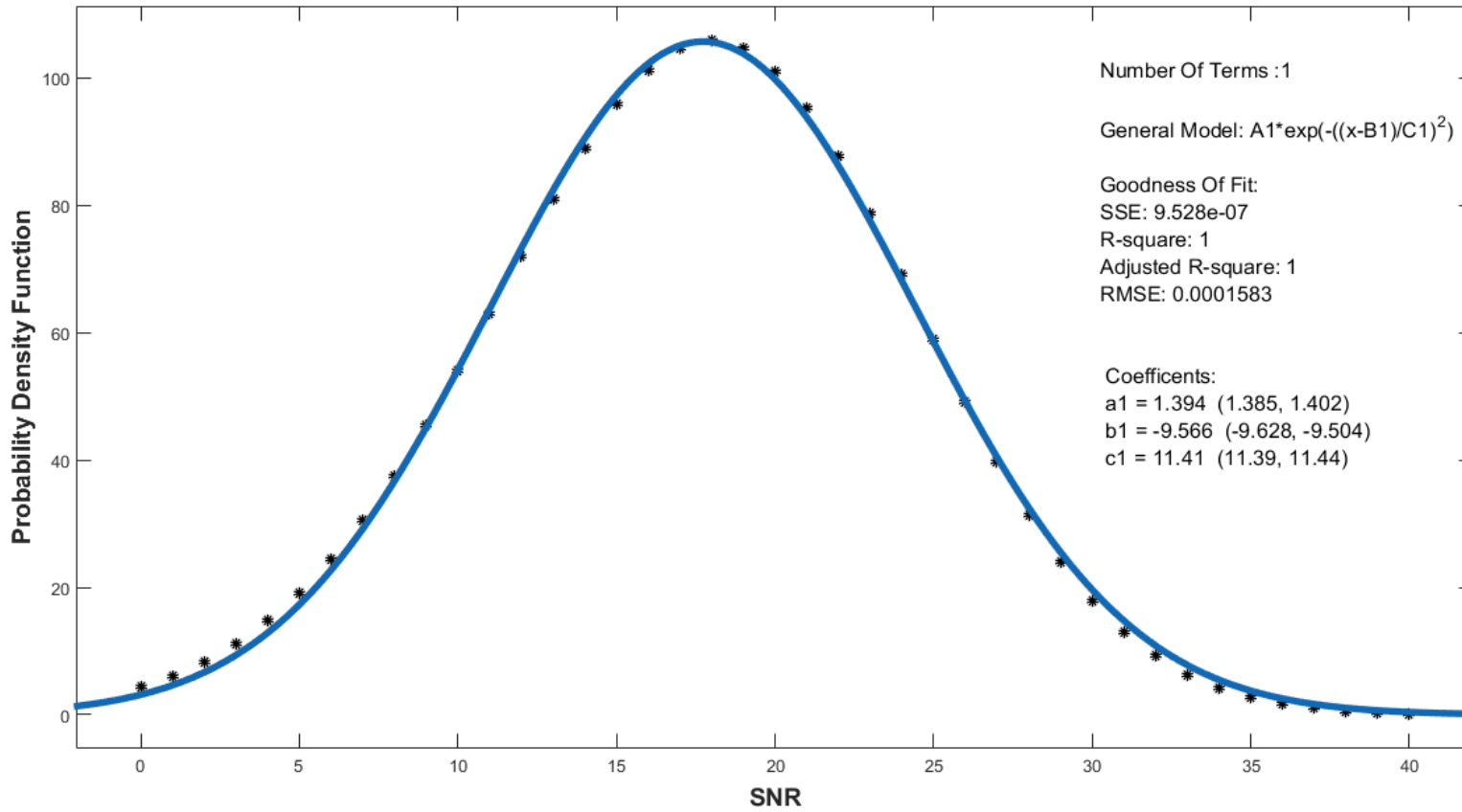


Figure 2 Gaussian Equation Model

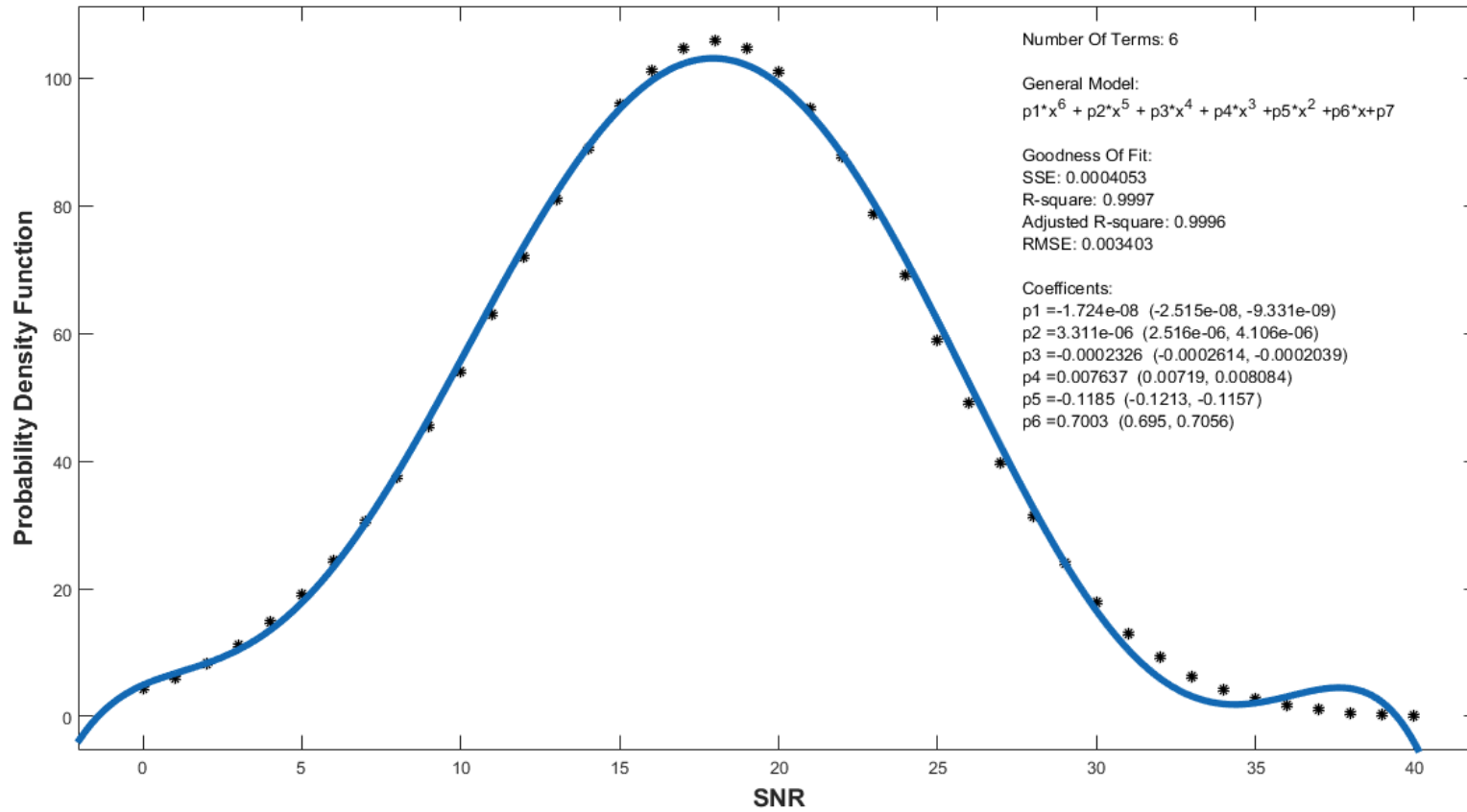


Figure 3 Polynomial Equation Model

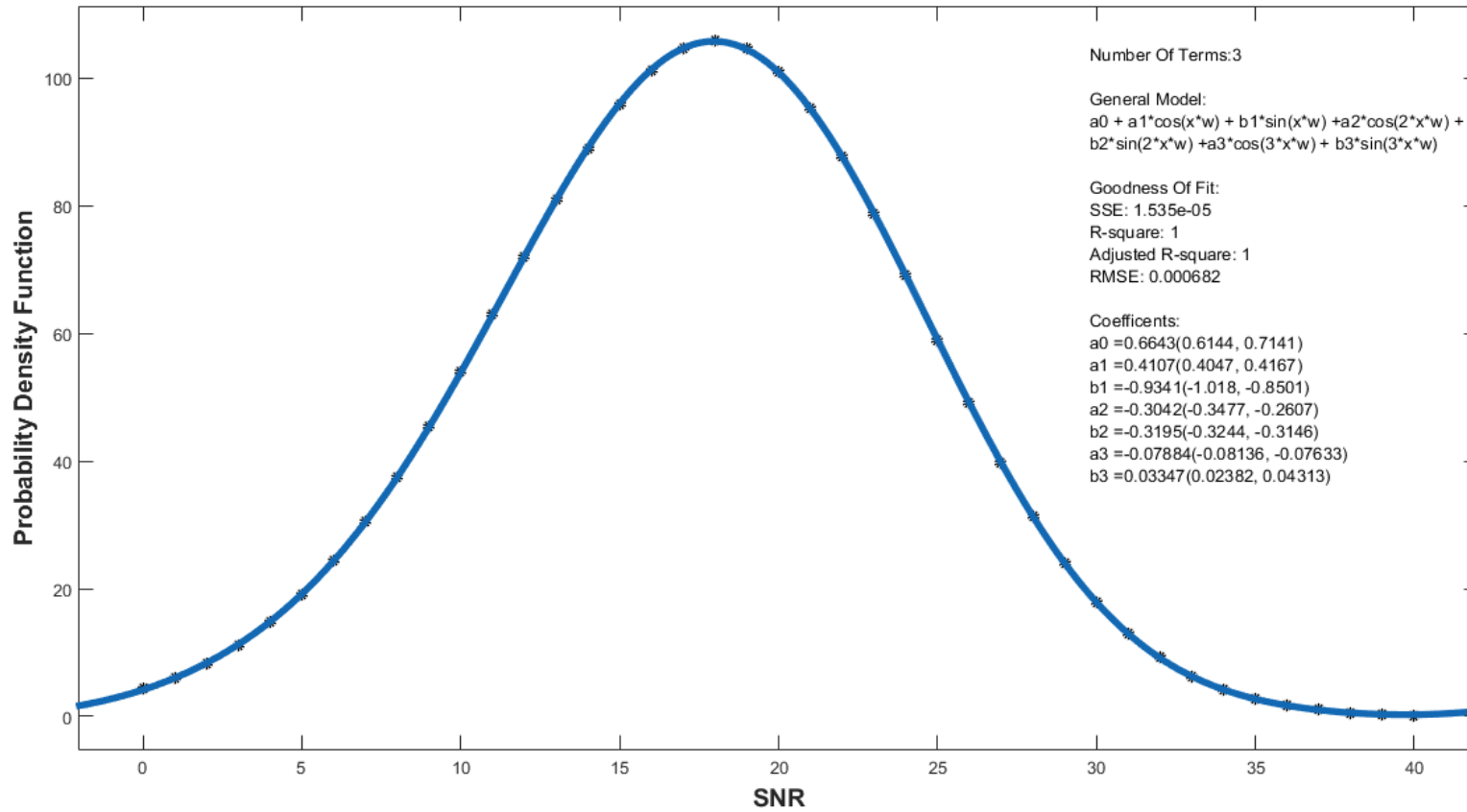


Figure 4 Fourier Equation Model

After we decide on the 1st degree Gaussian equation, instead of the complex $p(x)$ integral equation we use the Gaussian equation obtained from curve fitting utility of the MATLAB. That is, $p(x)$ in (2.15) is closely approximated by

$$p(x) = A * \exp\left(-\left(\frac{(X - B)}{C}\right)^2\right). \quad (2.16)$$

Thus using (2.16), we can calculate $p(x)$ more easily than complex integration form defined in equation (2.15). In the simple equation in (2.16), we have some coefficients A, B, C . We calculate these coefficients using MATLAB in the next part of thesis.

2.4 Coefficient Analyze According to Distance

In pursuit of this process we concentrate on the changes of A, B, C when we change distance L . In order to see this, we wrote a MATLAB code. The range value for L is 500 m to 2500 m, and for each L value, we calculate the A, B, C coefficients. After that, we plot the graphs of A, B, C with respect to L as indicated in Fig. 5, Fig. 6 and Fig. 7.

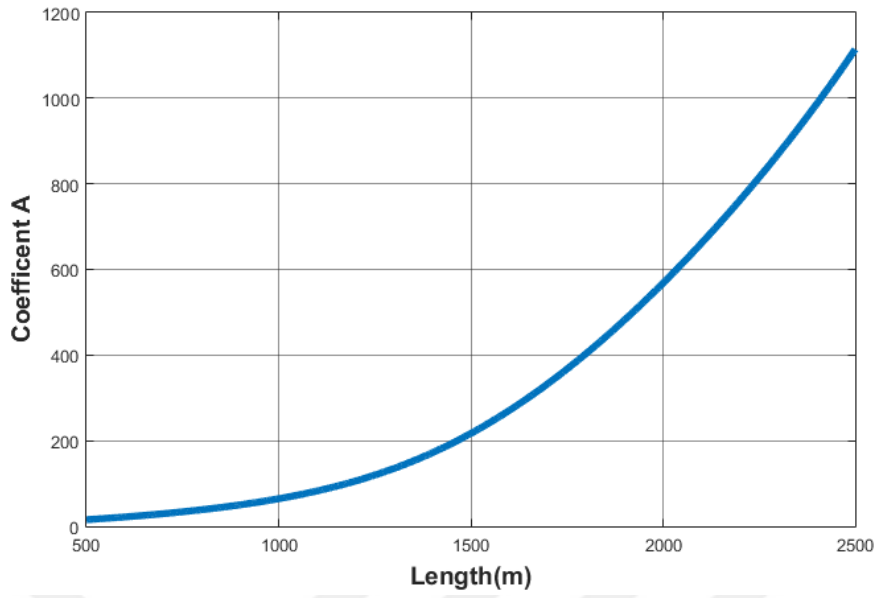


Figure 5 Change of A with respect to L

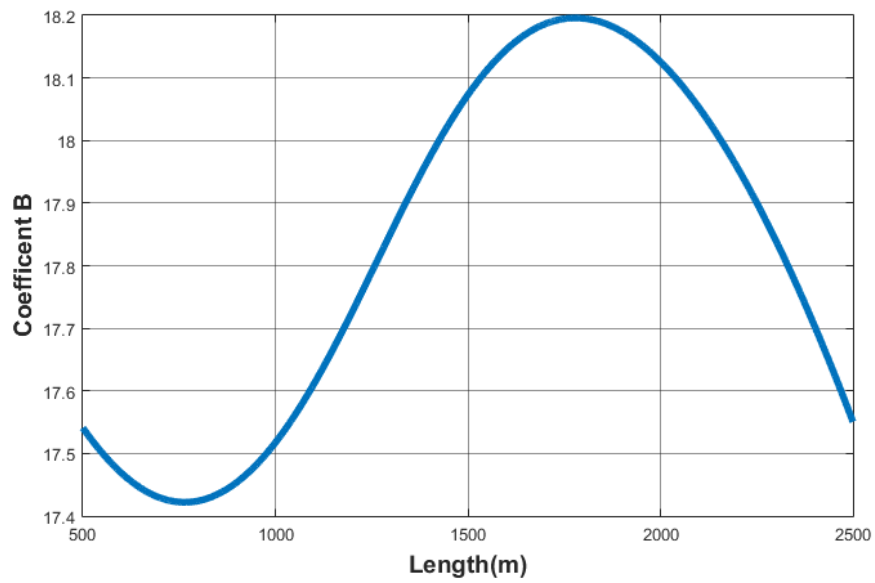


Figure 6 Change of B with respect to L

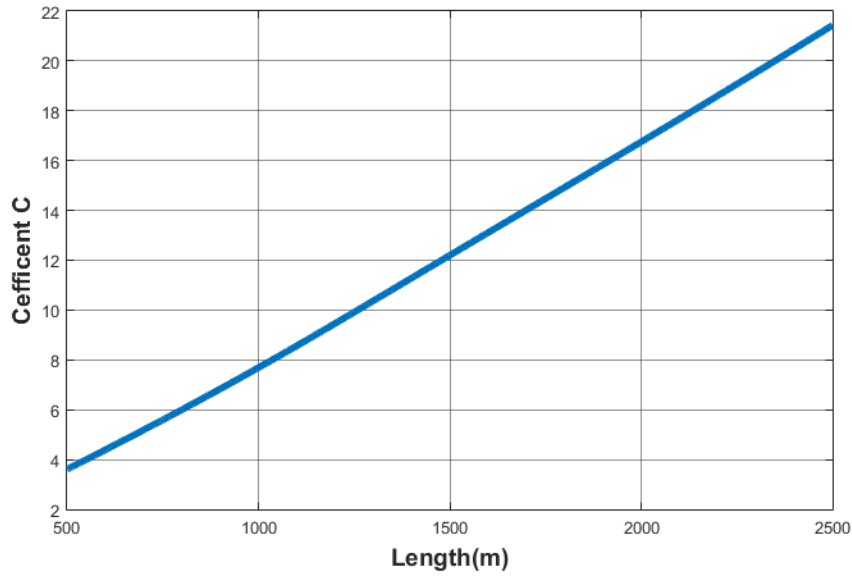


Figure 7 Change of C with respect to L

we inspect the change of the coefficients with distance. When we look at the results, A and C are increasing with distance but B is increasing until nearly 1500 meter. This means that the best distance is between 1000 and 1500 meter for our model. In next stage, we analyze how coefficients change with turbulence strength Cn^2 whose value depends on the σ variable in equation (2.5).

2.5 Coefficient Analyze According to Turbulence Strength

In this section, we inspect the change of A, B, C with Cn^2 which is the altitude – dependent turbulence strength varying from 10^{-17} to $10^{-13} m^{-2/3}$ according to the atmospheric turbulence conditions. Fifty different Cn^2 values ranging from 1.7×10^{-14} to $1.7 \times 10^{-13.5}$ are employed. We plot graph of A, B, C with respect to Cn^2 as in Fig.8, Fig. 9 and Fig. 10.

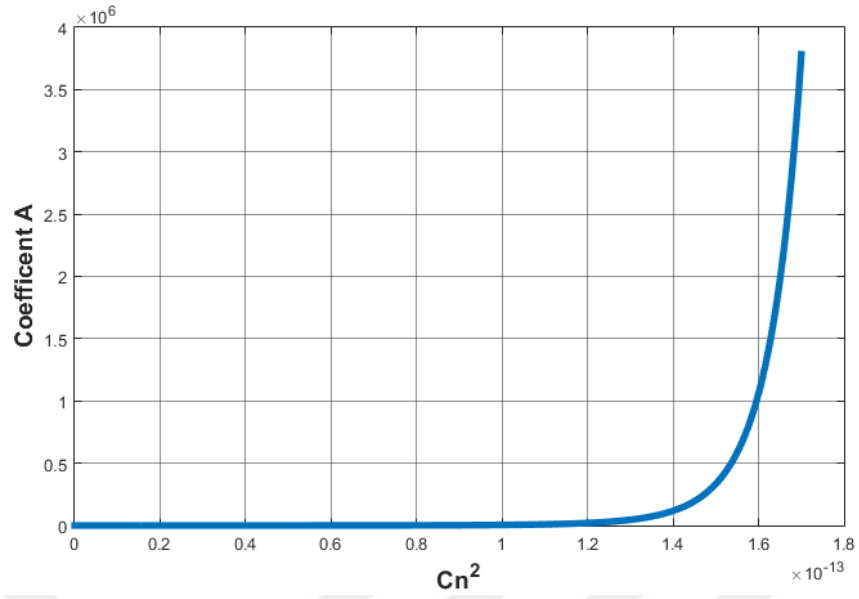


Figure 8 Change of A with respect to Cn^2

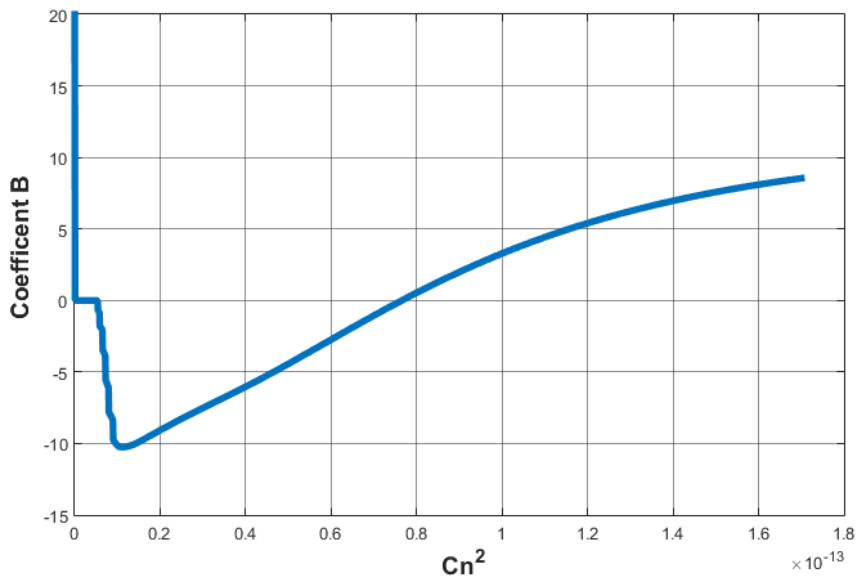


Figure 9 Change of B with respect to Cn^2

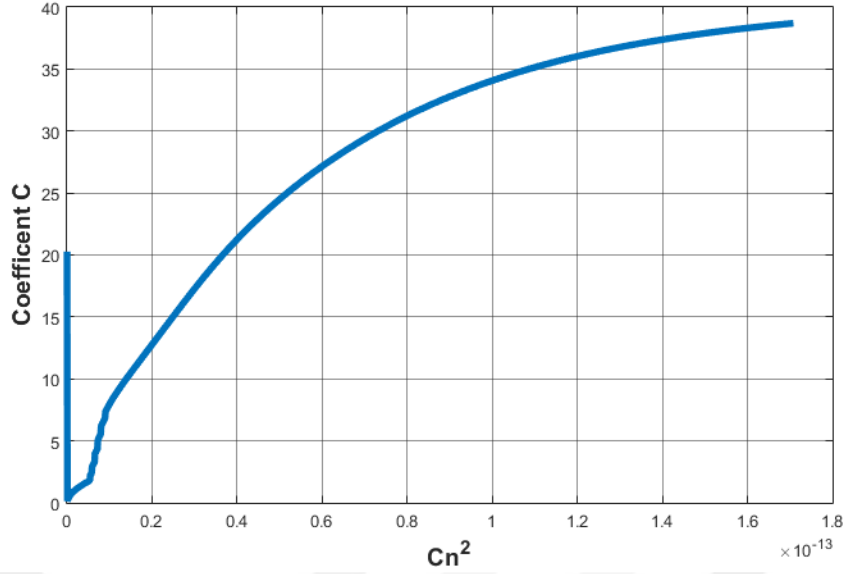


Figure 10 Change of C with respect to Cn^2

These graphs in Fig. 8, Fig. 9 and Fig. 10 mean that coefficient values increase in a regular manner when Cn^2 increases. This indicates that it is possible to relate the changes in the coefficients to the Cn^2 using the curve fitting utility of the MATLAB platform. In Table. 1 and Table 2, the coefficient values for different values of Cn^2 are tabulated.

We also inspect the change of the coefficients with regard to the changes in Cn^2 and L . We use 50 Cn^2 values ranging from 1.7×10^{-14} to $1.7 \times 10^{-13.5}$. The L values are chosen from 500 m to 2500 m . We implemented MATLAB's curve fitting options to these graphs. We detected best fitting option which is polynomial fitting in 6th degree for these graphs. After this fitting process, every graph is expressed via a polynomial equation in the form

$$p_1X^6 + p_2X^5 + p_3X^4 + p_4X^3 + p_5X^2 + p_6X^1 + p_7. \quad (2.17)$$

We determined the coefficients of the polynomials for every Cn^2 . For the calculation of $p(x)$, we need to know Cn^2 and L . If we have these values, we can find the coefficient values of the polynomial from the table of Table 1 and Table 2.

In Fig. 11, we plot the graphs of the coefficients with respect to the changes in Cn^2 . We obtained 21 graphs for all coefficient values. In Fig. 11, first row refers to the coefficients of the polynomial modeling of A , i.e., refers to the coefficients $A - p1$ to $A - p7$, similarly the second row refers to $B - p1$ to $B - p7$ and third row refers $C - p1$ to $C - p7$ respectively.



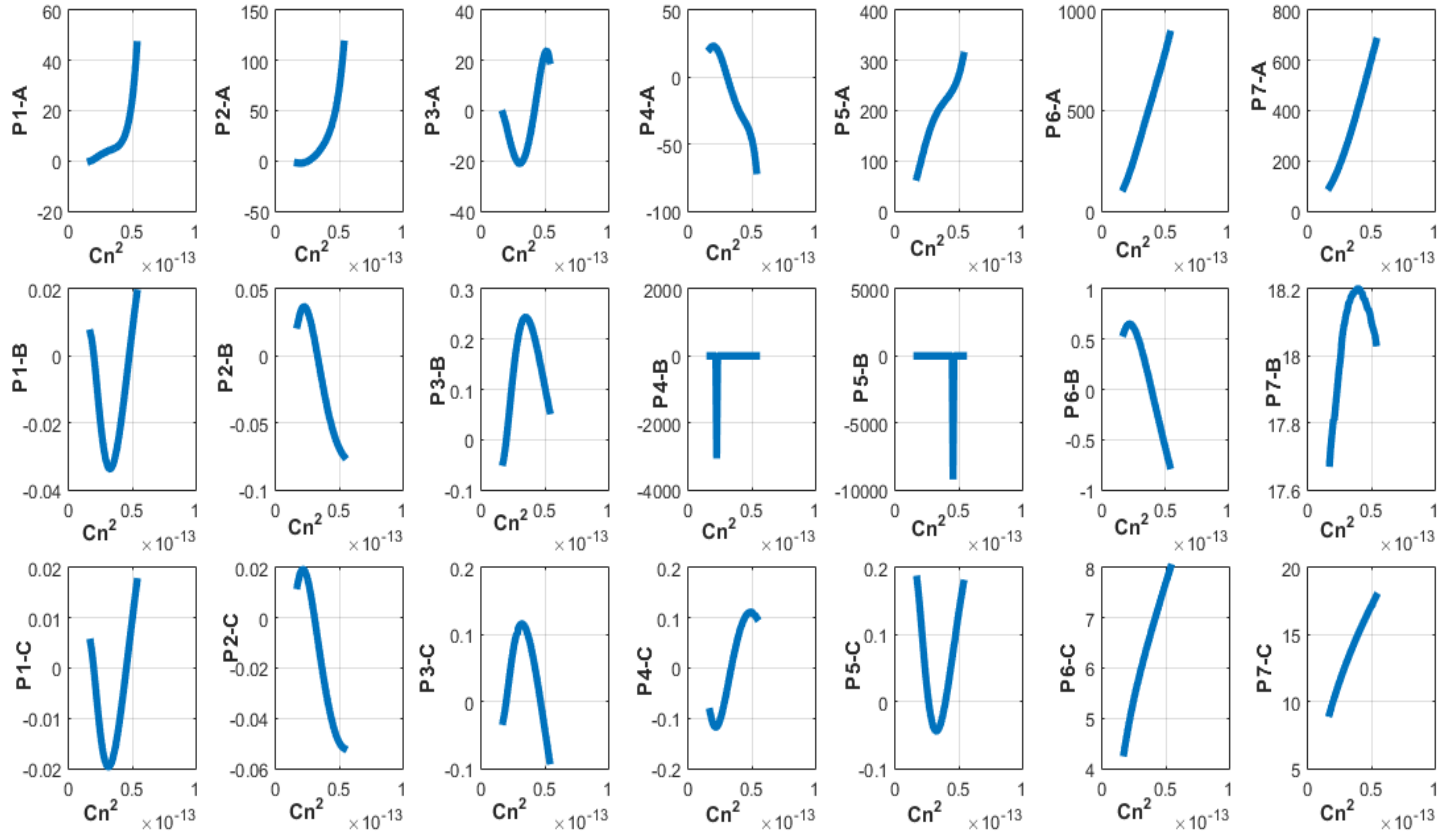


Figure 11 Polynomial Equation Coefficient Values to Cn^2 Graphs.

2.6 Comparison MATLAB Model and Integral Form of Probability Density Function

Considering all these processes we can claim that our simple equation which is expressed in (2.15) can be used instead of the complex integral equation which is defined in (2.16). For this comparison, we wrote a MATLAB code where we calculate both equations and plot their graphs as in Fig. 12. It is shown in Fig. 12 that our model and the original equation fit to each other very well.

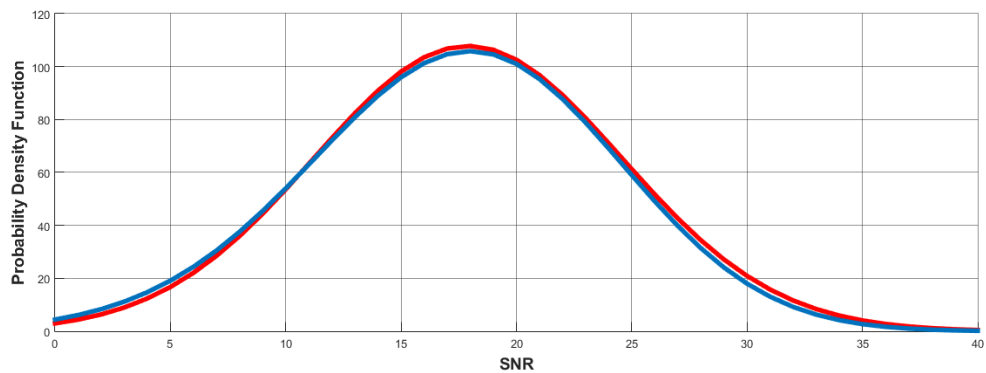


Figure 12 Comparison of Result

In Fig. 12, red line was obtained from MATLAB model. Blue line was obtained from integral equation. As we see, both lines nearly overlap to each other. That means we can use equation (2.16) instead of equation (2.15). The developed expression is in closed form and it can be evaluated more easily.

CHAPTER 3

Calculations of Functions

3.1 Cumulative Distribution Function (CDF)

The cumulative distribution function for the log normal distribution model is obtained by integrating the probability density function of the log normal model ($Prob.(x^2 < x)$). We obtain probability density function from MATLAB model which is given by (2.16).

$$CDF = \int_0^x p(x) dx \quad (3.1)$$

Using equation (2.16) we can calculate the cumulative density function as in (3.2).

$$CDF = \int_0^x A \exp - \left(\frac{X - B}{C} \right)^2 dx \quad (3.2)$$

The error function is defined as in (3.3)

$$\emptyset(u) = \text{erf}(u) = \frac{2}{\pi} \int_0^u e^{-x^2} dx. \quad (3.3)$$

We employ the error function in (3.3) for the pdf expression in (2.15) For this purpose, we write U instead of X as defined in equation (3.4) and after that we make some transformation for simple calculation of error function as in (3.5).

$$CDF = \int_0^x A \exp - \left(\frac{U - B}{C} \right)^2 du . \quad (3.4)$$

$$y = (U - B)/C \quad dy = \left(\frac{1}{c}\right) du. \quad (3.5)$$

After transformation of the cumulative distribution function we obtain a simpler equation as shown in (3.6). The defined limit of integral is divided into two parts as shown in equation (3.7).

$$CDF = \int_{-\frac{B}{C}}^{\frac{x-B}{C}} A e^{-y^2} C dy \quad (3.6)$$

$$CDF = AC \left[\int_{(-\frac{B}{C})}^0 e^{-y^2} dy + \int_0^{\frac{x-B}{C}} e^{-y^2} dy \right] \quad (3.7)$$

3.2 Moment Generating Function (MGF)

The n degree moment of a random variable X is defined as $E[X^n]$. For example, the first moment is the expected value $E[X]$. The second central moment is the variance of X . Similar to mean and variance, other moments give useful information about random variables. The moment generating function (MGF) of a random variable X is a function $M_x(s)$ defined as

$$M_x(s) = E(e^{sx}) = \int_0^{\infty} P(x) e^{sx} dx \quad (3.8)$$

and for our proposed model, the moment generating function is calculated as

$$M_x(s) = A e^{-\left(\frac{B^2}{C^2}\right)} \int_0^{\infty} e^{\left(\left(-\frac{x^2}{C^2}\right)+x\left(\left(\frac{2B}{C^2}\right)+s\right)\right)} dx \quad (3.9)$$

Which can be expressed in closed form using the $\phi(\cdot)$ function defined in [7, Eq. (3.322.2)] as

$$M_x(s) = A e^{-\left(\frac{B^2}{C^2}\right)} \sqrt{\left(\frac{\pi C^2}{4}\right)} \exp\left(-\left(\frac{C^2}{4}\right)\right) \left(\left(\frac{2B}{C^2}\right) + s\right)^2 \left[1 - \phi - \left(\left(\frac{2B}{C^2}\right) + s\right) \sqrt{\frac{C^2}{4}} \right] \quad (3.10)$$

3.3 Moments

The “moments” of a random variable (or of its distribution) are expected values of powers or related functions of the random variable. Moments of the two signals for log normal distribution are calculated in equation (3.11),(3.12), (3.13) and (3.14).

$$E(X^n) = \frac{d^n}{ds^n} M(s)|_{s=0} \quad (3.11)$$

$$\Phi\left(-\left(\frac{2B}{C^2} + S\right)\right)^{\frac{C}{2}} = \frac{2}{\sqrt{\pi}} \int_0^{\left(-\frac{2B}{C^2} + S\right)^{\frac{C}{2}}} e^{-x^2} dx \quad (3.12)$$

$$\frac{d}{ds} \left(\frac{2}{\sqrt{\pi}} \int_0^{\left(-\frac{2B}{C^2} + S\right)^{\frac{C}{2}}} e^{-x^2} dx \right) = -\frac{2}{\sqrt{\pi}} e^{\left(-\frac{2B}{C^2} + S\right)^{\frac{C}{2}}} \frac{C}{2} \quad (3.13)$$

$$\frac{dM(s)}{ds} |_{s=0} = A e^{-\frac{B^2}{C^2}} \frac{\sqrt{\pi C^2}}{4} \left[\exp\left(\frac{B^2}{C^2}\right) B \right] \left[1 - \Phi\left(-\frac{B}{C}\right) \right] + \exp\left(\frac{B^2}{C^2}\right) \left(\frac{2}{\sqrt{\pi}} \frac{C}{2} e^{-\frac{B^2}{C^2}} \right) \quad (3.14)$$

3.4 Outage Probability

The outage probability is defined as the probability that the SNR at the input of the receiver chain is falling below a given threshold value. Outage probability of our model is calculated in equation (3.15) and (3.16) .

$$P_\gamma = 2P(2x) \quad P(x) = A \exp(-(x - B)/C^2) \quad (3.15)$$

$$P_\gamma = 2A \exp(-(2x - B)/C^2) \quad (3.16)$$

3.5 Amount of Fading

The amount of fading is an important measure for severity of fading and it is defined as [10, Eq. (2.5)]

$$AF = \frac{(E(\tau^2) - (E(\tau))^2)}{E(\tau^2)} \quad (3.17)$$

For the calculation of (3.17), we first compute $E(\tau^2)$ as outlined in (3.19), (3.20) and (3.21).

$$E(\tau^2) = \int_0^{\infty} \tau^2 P(\tau) d\tau \rightarrow P(\tau) = A * \exp\left(-\left(\frac{(\tau - B)}{C}\right)^2\right) \quad (3.18)$$

$$k = \frac{(\tau - B)}{C} \rightarrow \tau = Ck + B \rightarrow d\tau = Cdk \quad (3.19)$$

$$E(\tau^2) = \int_0^{\infty} (Ck + B)^2 A e^{-k^2} C dk \quad (3.20)$$

$$E(\tau^2) = \int_0^{\infty} AC^3 k^2 e^{-k^2} dk + \int_0^{\infty} 2ABC^2 k e^{-k^2} dk + \int_0^{\infty} AB^2 C e^{-k^2} dk \quad (3.21)$$

\Leftrightarrow
W

\Leftrightarrow
X

\Leftrightarrow
Y

$$\int_{-\infty}^{\infty} e^{-\frac{\tau^2}{2}} dy = \sqrt{2\pi} \rightarrow -\frac{\tau^2}{2} = x^2 \rightarrow x = \frac{\tau}{\sqrt{2}} \rightarrow dx = 1/\sqrt{2}d\tau \quad (3.22)$$

$$E(\tau^2) = \int_{-\infty}^{\infty} e^{-x^2} \sqrt{2} dx = \sqrt{2\pi} \rightarrow \int_{-\infty}^{\infty} e^{-x^2} dx = \sqrt{\pi} \quad (3.23)$$

Integration by parts is a technique for performing indefinite integration $\int u dv$ or definite integration

$$\int_a^b u \, dv$$

by expanding the differential of a product of functions $d(u, v)$ and expressing the original integral in terms of a known integral $\int v \, du$. We made this transformation in equation (3.25) and (3.27).

For the W part of equation (3.21), we have

$$\int_0^\infty AC^3 k^2 e^{-k^2} dk = AB^2 C \sqrt{\pi} \quad (3.24)$$

For the X part of equation (3.21),

$$\int_0^\infty 2ABC^2 k e^{-k^2} dk \rightarrow -k^2 = u \quad du = -2k dk \quad (3.25)$$

$$-\int_0^\infty ABC^2 e^{-u} du = -ABC^2 e^{-\left(\frac{\tau-B}{C}\right)^2} \quad (3.26)$$

For the Y part of equation (3.21), we have

$$\begin{aligned} \int_0^\infty AC^3 k^2 e^{-k^2} dk \rightarrow k^2 = u \rightarrow k = \sqrt{u} \rightarrow du = 2k dk \rightarrow e^{-k^2} dk = dv \\ \rightarrow v = \sqrt{\pi} \end{aligned} \quad (3.27)$$

$$\int_0^\infty \frac{1}{2k} AC^3 u e^{-u} du = k^2 \sqrt{\pi} - \int_0^\infty 2\sqrt{\pi} k dk = 0 \quad (3.28)$$

At the end of transformation and calculation we can calculate $E(\tau^2)$ as shown in(3.29).

$$E(\tau^2) = AB^2C\sqrt{\pi} - ABC^2e^{-\left(\frac{\tau-B}{C}\right)} \quad (3.29)$$

Second, we calculate $E(\tau)$ for the amount of fading as in equation (3.31), (3.32),(3.33),(3.34).

$$E(\tau) = \int_0^\infty \tau A e^{-\left(\frac{\sqrt{\tau}-B}{C}\right)^2} \quad (3.30)$$

$$E(\tau) = \int_0^\infty (C^2k^2 + 2BCk + B^2) A e^{-k^2} (2C^2k + 2BC) dk \quad (3.31)$$

$$\left(\frac{\sqrt{\tau}-B}{C}\right) = k \rightarrow \tau = C^2k^2 + 2BCk + B^2 \rightarrow d\tau = 2C^2k + 2BC dk \quad (3.32)$$

$$E(\tau) = \int_0^\infty \underset{A}{2AC^4k^3e^{-k^2} dk} + \int_0^\infty \underset{B}{2AC^4k^3e^{-k^2} dk} + \int_0^\infty \underset{C}{2AC^4k^3e^{-k^2} dk} + \int_0^\infty \underset{D}{2AC^4k^3e^{-k^2} dk} \quad (3.33)$$

For the A part of equation (3.33),

$$\int_0^\infty 2AC^4k^3e^{-k^2} dk = 0 \quad (3.34)$$

For the B part of equation (3.33),

$$\int_0^\infty 6ABC^3k^2e^{-k^2} dk = 0 \quad (3.35)$$

For the C part of equation (3.33), we have

$$\int_0^{\infty} 6AB^2C^2ke^{-k^2} dk = -3AB^2C^2e^{-\left(\frac{\tau-B}{C}\right)^2} \quad (3.36)$$

For the D part of equation (3.33),

$$\int_0^{\infty} 2AB^3C e^{-k^2} dk = 2AB^3C\sqrt{\pi} \quad (3.37)$$

At the end of the all calculation $E(\tau)$ is equal to,

$$E(\tau) = 2AB^3C\sqrt{\pi} - 3AB^2C^2e^{-\left(\frac{\tau-B}{C}\right)^2}. \quad (3.38)$$

Now, we have all parameters to calculate the amount of fading which is expressed in (3.17). If we apply our calculated parameters to formula (3.17), amount of fading formula becomes as in (3.39).

$$AF = \frac{\left[AB^2C\sqrt{\pi} - ABC^2e^{-\left(\frac{\tau-B}{C}\right)^2}\right] - \left[2AB^3C\sqrt{\pi} - 3AB^2C^2e^{-\left(\frac{\tau-B}{C}\right)^2}\right]}{\left[2AB^3C\sqrt{\pi} - 3AB^2C^2e^{-\left(\frac{\tau-B}{C}\right)^2}\right]} \quad (3.39)$$

3.6 Probability of Transmission Error Rate

In the last stage of thesis work, we calculate the probability of transmission error rate performance of the log-normal channels using our model. The modeling of the probability density function is done with $\bar{\mu} = 15$. Now we consider the values of $\bar{\mu}$ from 5 up to 40 with incremental amount of 5. We perform the same steps until Fig. 7. We calculate $p(x)$ of the harmonic mean and we plot its graph. Then, using MATLAB, we model the change of coefficients A, B, C for all $\bar{\mu}$ values. We plot the graphs of A, B, C coefficients with respect to L . Then, we use curve fitting option of MATLAB again and calculate polynomial coefficient for these graphs. The best fitting curve is achieved using a 6th degree polynomial. Polynomial equations of A, B, C graphs become as in (3.39) after fitting operation.

$$p_1X^6 + p_2X^5 + p_3X^4 + p_4X^3 + p_5X^2 + p_6X^1 + p_7 \quad (3.39)$$

This is a general polynomial equation with constant coefficients. We obtain these equations for each $\bar{\mu}$ value. Subsequently, we compare the models which are expressed by equation (2.15) and (2.16). We plot graphs for both equations with different $\bar{\mu}$ values on the same figure. Blue line is obtained from integral equation and red line is generated from our model.

For $\bar{\mu} = 5$, coefficients of polynomial equations are given in (3.42). Graphs of A , B and C coefficients with respect to length are depicted in Fig. 13, 14 and 15. We plot the pdf obtained using the numerical integration and the one obtained using the modeling technique presented in this thesis work for $\bar{\mu} = 5$ in Fig. 16.

$$p1X^6 + p2X^5 + p3X^4 + p4X^3 + p5X^2 + p6X^1 + p7.$$

A▶	P1	P2	P3	P4	P5	P6	P7	
	-0.1913	-0.5432	3.294	17.11	33.33	38.05	23.5	
B▶	P1	P2	P3	P4	P5	P6	P7	
	0.00034	0.03009	0.01087	-0.278	0.088	1.312	8.45	
C▶	P1	P2	P3	P4	P5	P6	P7	
	0.00996	0.02523	-0.0743	-0.159	0.369	5.539	12.0	(3.42)

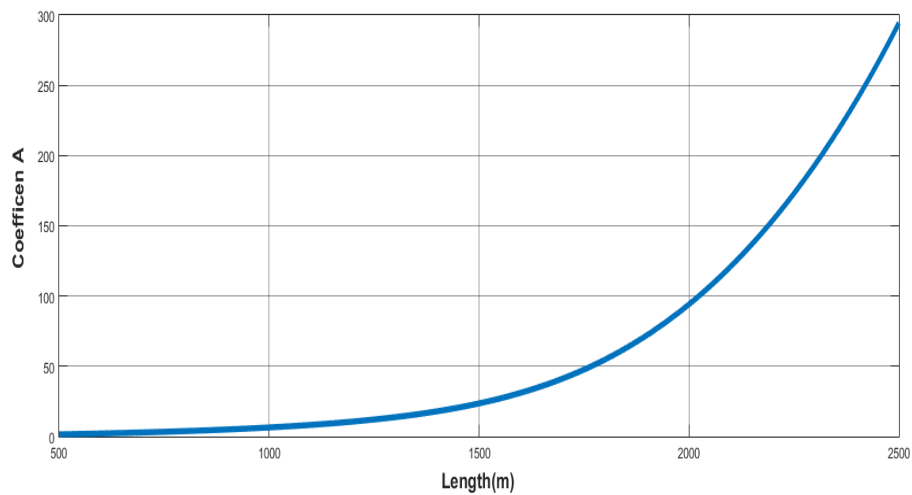


Figure 13 Change of A with respect to L for $\bar{\mu} = 5$

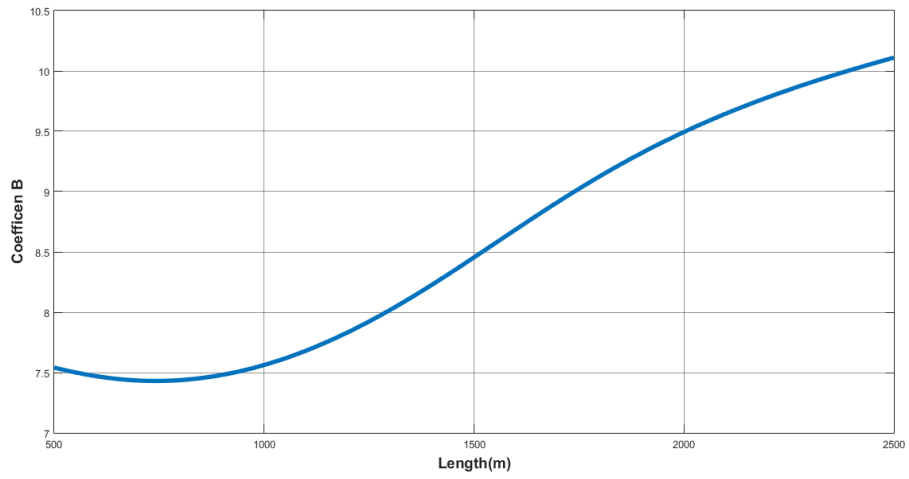


Figure 14 Change of B with respect to L for $\bar{\mu} = 5$

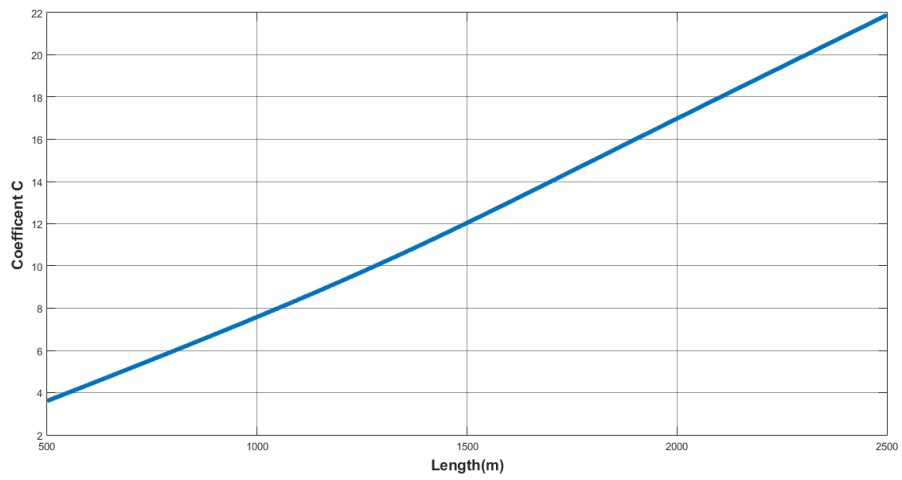


Figure 15 Change of C with respect to L for $\bar{\mu} = 5$

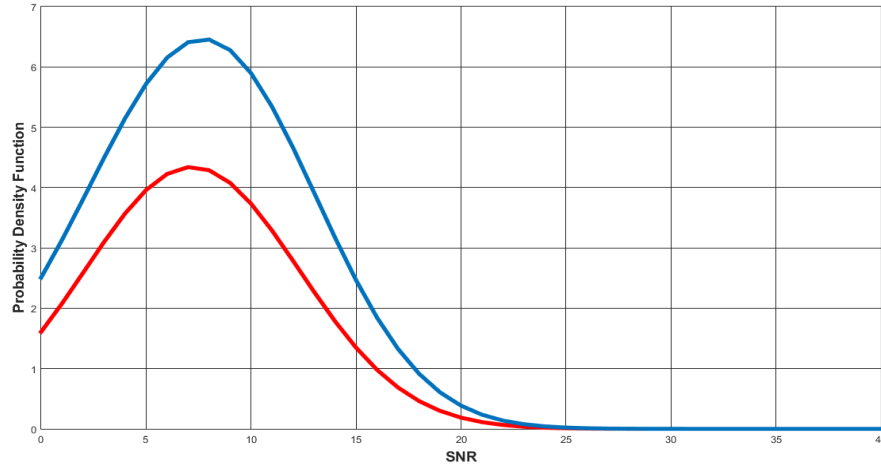


Figure 16 Comparisons of Results for $\bar{\mu} = 5$

For $\bar{\mu} = 10$, coefficients of polynomial equations are given in (3.43). Graphs of A , B and C coefficients with respect to length are depicted in Fig. 17, 18 and 19. We plot the pdf obtained using the numerical integration and the one obtained using the modeling technique presented in this thesis work for $\bar{\mu} = 10$ in Fig. 20.

$$p1X^6 + p2X^5 + p3X^4 + p4X^3 + p5X^2 + p6X^1 + p7.$$

A ▶	P1	P2	P3	P4	P5	P6	P7	
	0.5269	-1.274	-2.794	23.59	79.26	110.5	72.91	
B ▶	P1	P2	P3	P4	P5	P6	P7	
	-0.0099	0.0334	0.0736	-0.297	-0.150	0.985	13.27	
C ▶	P1	P2	P3	P4	P5	P6	P7	
	-0.0017	0.0184	0.0117	-0.123	0.1307	5.432	12.2	(3.43)

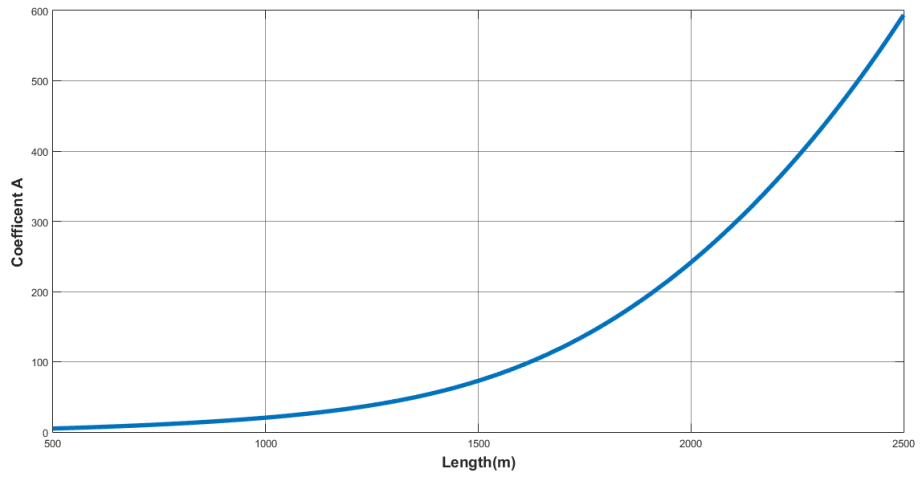


Figure 17 Change of A with respect to L for $\bar{\mu} = 10$

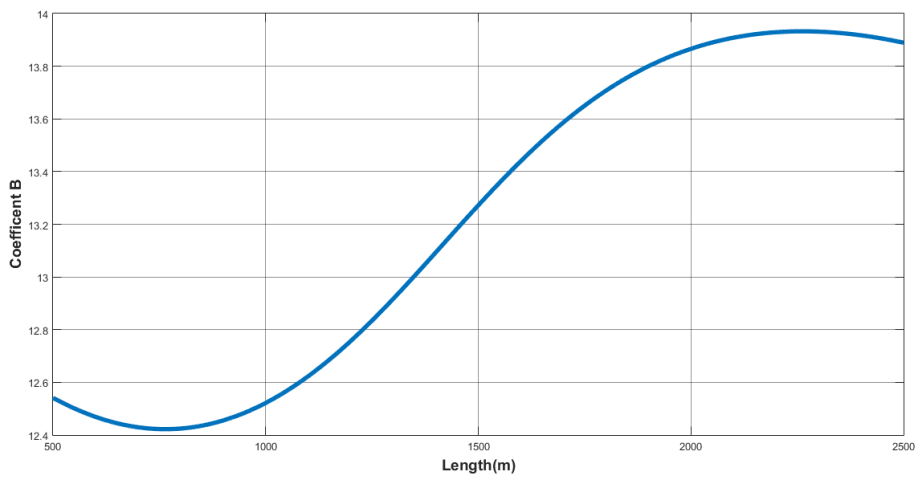


Figure 18 Change of B with respect to L for $\bar{\mu} = 10$

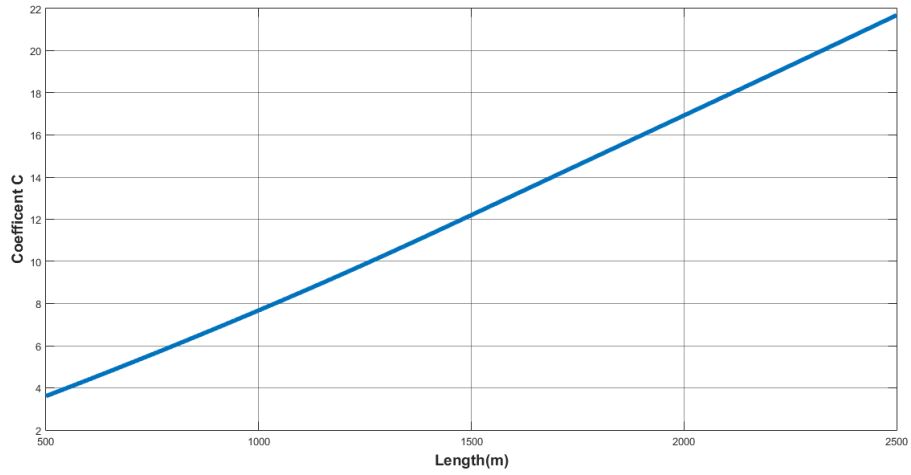


Figure 19 Change of C with respect to L for $\bar{\mu} = 10$

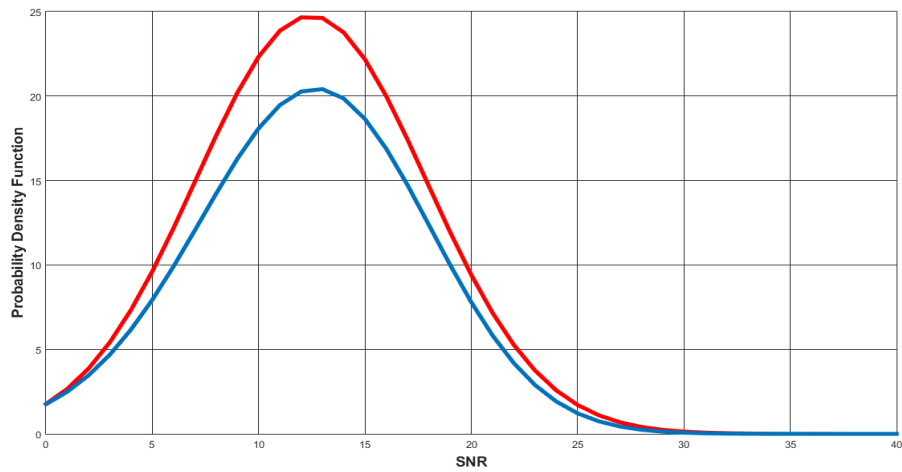


Figure 18 Comparisons of Results for $\bar{\mu} = 10$

For $\bar{\mu} = 15$, coefficients of polynomial equations are given in (3.44). Graphs of A , B and C coefficients with respect to length are depicted in Fig. 21, 22 and 23. We plot the pdf obtained using the numerical integration and the one obtained using the modeling technique presented in this thesis work for $\bar{\mu} = 15$ in Fig. 24.

$$p1X^6 + p2X^5 + p3X^4 + p4X^3 + p5X^2 + p6X^1 + p7.$$

A ▶	P1	P2	P3	P4	P5	P6	P7	
	2.131	1.015	-15.16	7.957	142.6	0.508	18.07	
B ▶	P1	P2	P3	P4	P5	P6	P7	
	-0.0196	0.0183	0.1415	-0.223	-0.4255	0.508	18.07	
C ▶	P1	P2	P3	P4	P5	P6	P7	
	-0.0124	0.0067	0.0792	-0.064	-0.0183	5.27	12.19	(3.44)

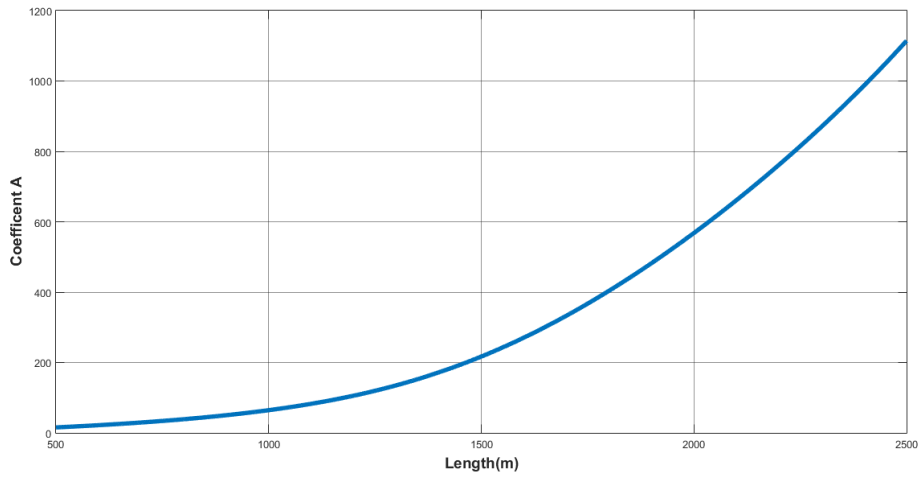


Figure 19 Change of A with respect to L for $\bar{\mu} = 15$

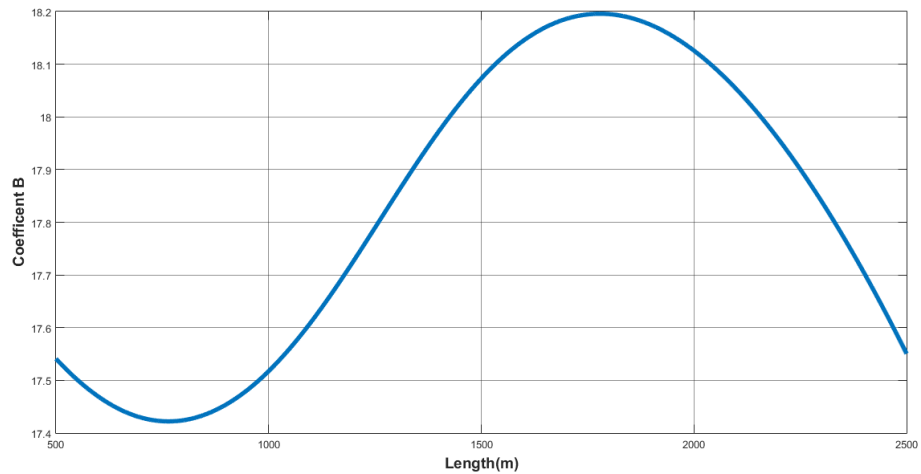


Figure 20 Change of B with respect to L for $\bar{\mu} = 15$

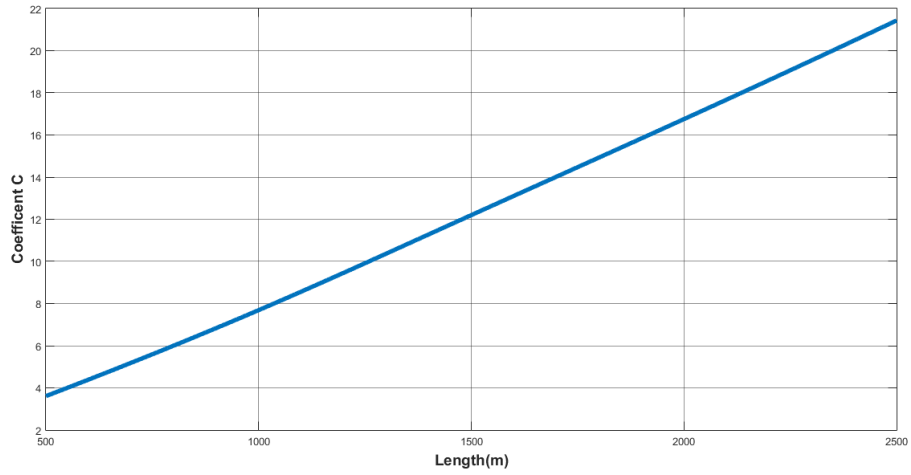


Figure 21 Change of C with respect to L for $\bar{\mu} = 15$

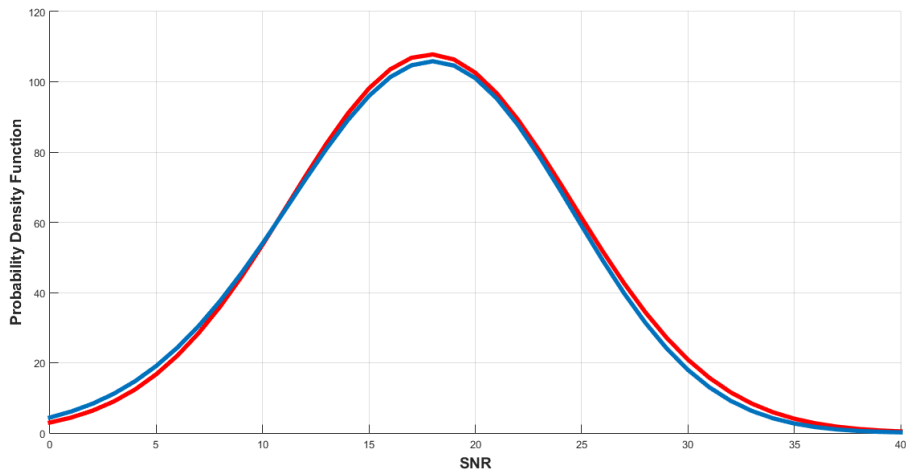


Figure 22 Comparisons of Results for $\bar{\mu} = 15$

For $\bar{\mu} = 20$, coefficients of polynomial equations are given in (3.45). Graphs of A , B and C coefficients with respect to length are depicted in Fig. 25, 26 and 27. We plot the pdf obtained using the numerical integration and the one obtained using the modeling technique presented in this thesis work for $\bar{\mu} = 20$ in Fig.28.

$$p1X^6 + p2X^5 + p3X^4 + p4X^3 + p5X^2 + p6X^1 + p7.$$

A ▶	P1	P2	P3	P4	P5	P6	P7	
	0.8672	9.388	-7.229	-50.57	144.6	614.3	601.7	
B ▶	P1	P2	P3	P4	P5	P6	P7	
	-0.0177	-0.008	0.149	-0.080	-0.5987	-0.110	22.74	
C ▶	P1	P2	P3	P4	P5	P6	P7	(3.45)
	-0.0043	-0.008	0.0380	0.0259	0.0389	5.059	12.03	

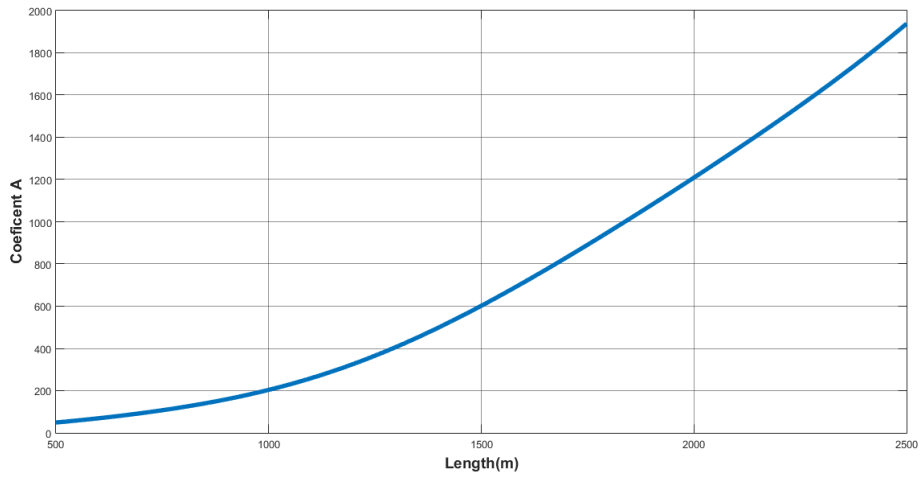


Figure 23 Change of A with respect to L for $\bar{\mu} = 20$

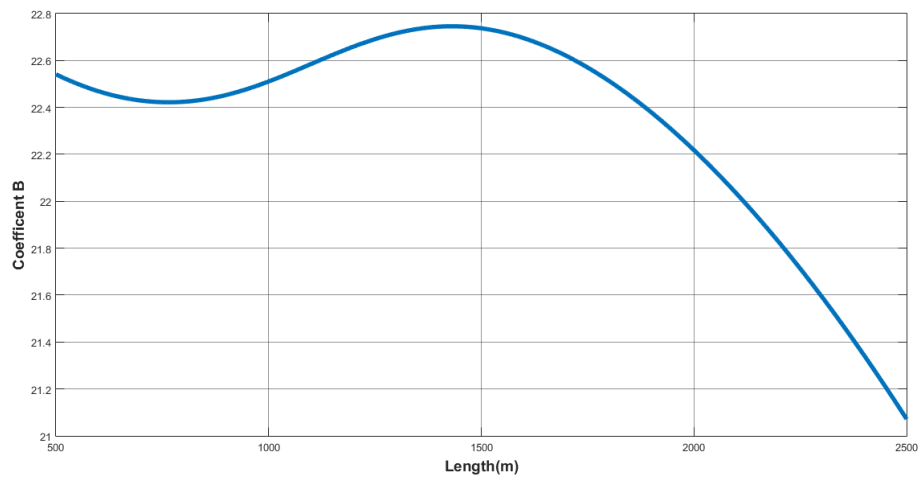


Figure 24 Change of B with respect to L for $\bar{\mu} = 20$

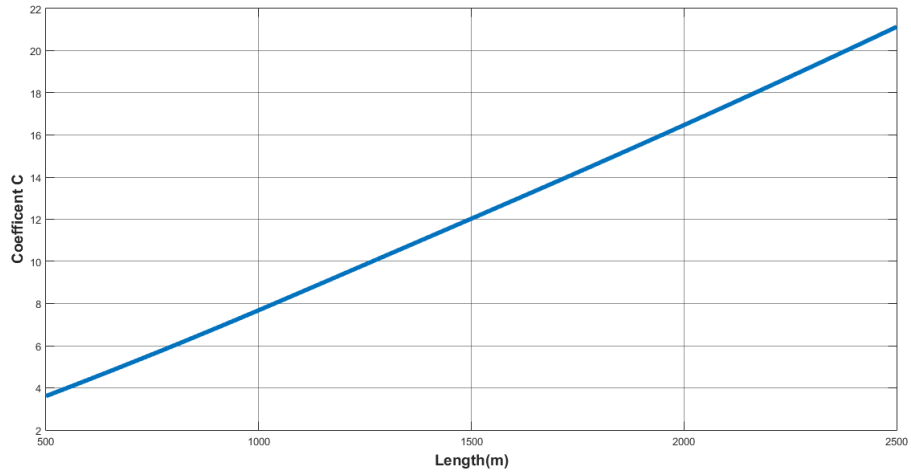


Figure 25 Change of C with respect to L for $\bar{\mu} = 20$

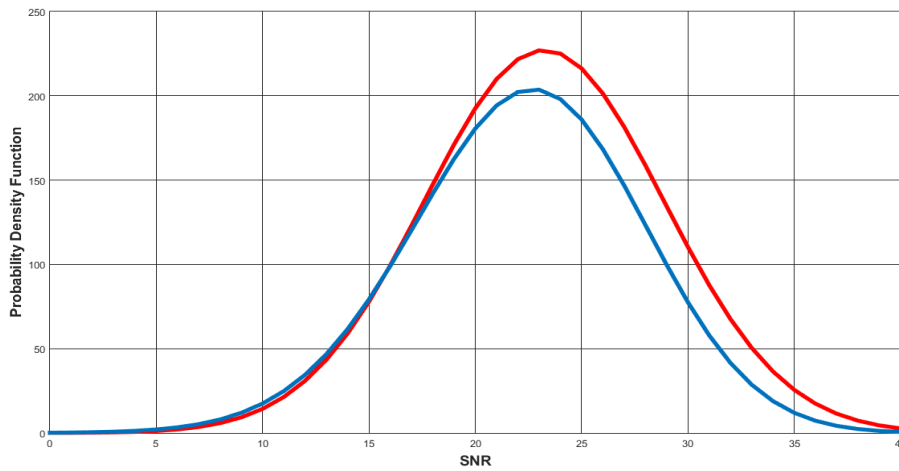


Figure 26 Comparisons of Results for $\bar{\mu} = 20$

For $\bar{\mu} = 25$, coefficients of polynomial equations are given in (3.46). Graphs of A , B and C coefficients with respect to length are depicted in Fig. 29, 30 and 31. We plot the pdf obtained using the numerical integration and the one obtained using the modeling technique presented in this thesis work for $\bar{\mu} = 25$ in Fig.32.

$$p1X^6 + p2X^5 + p3X^4 + p4X^3 + p5X^2 + p6X^1 + p7.$$

A▶	P1	P2	P3	P4	P5	P6	P7	
	-7.749	11.57	61.63	-90.19	-68.04	1020	1483	
B▶	P1	P2	P3	P4	P5	P6	P7	
	0.0010	-0.0298	0.0506	0.0608	-0.548	-0.821	27.15	
C▶	P1	P2	P3	P4	P5	P6	P7	
	0.0070	-0.0185	-0.031	0.1034	0.180	4.813	11.75	(3.46)

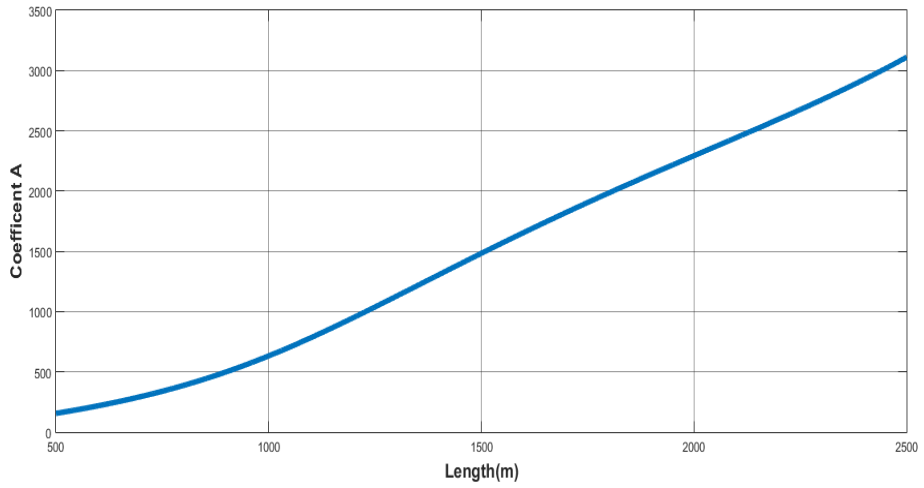


Figure 27 Change of A with respect to L for $\bar{\mu} = 25$

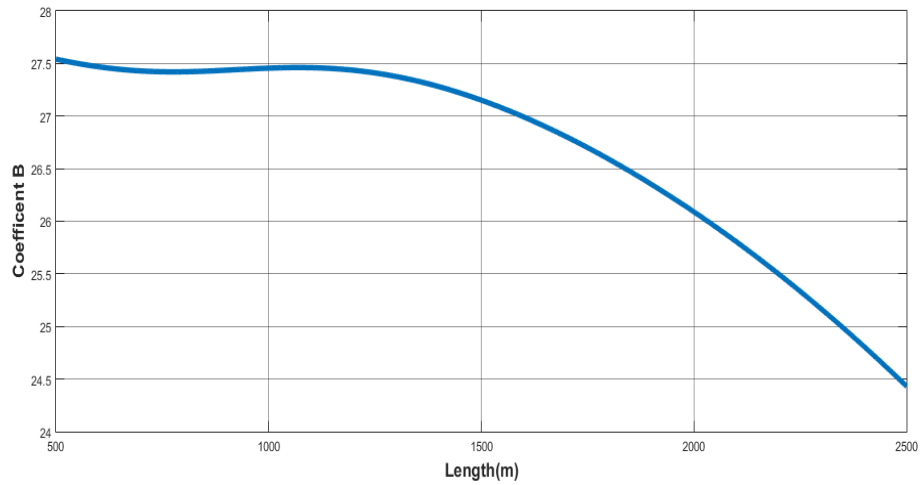


Figure 28 Change of B with respect to L for $\bar{\mu} = 25$

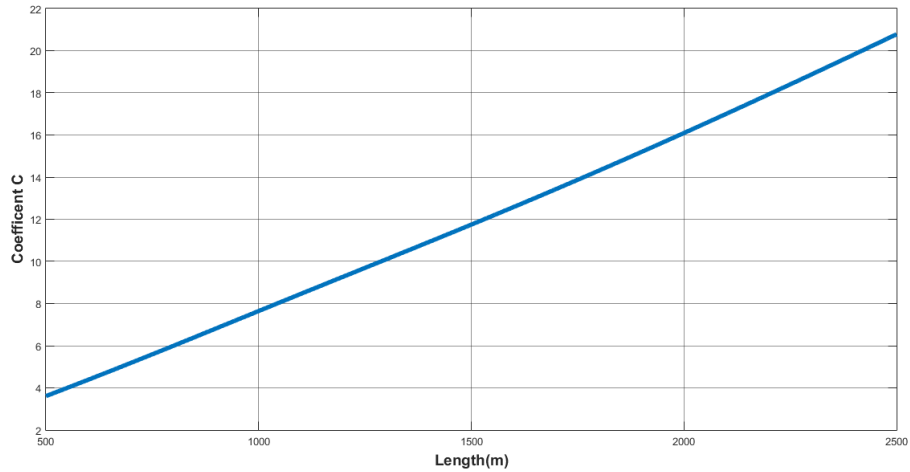


Figure 29 Change of C with respect to L for $\bar{\mu} = 25$

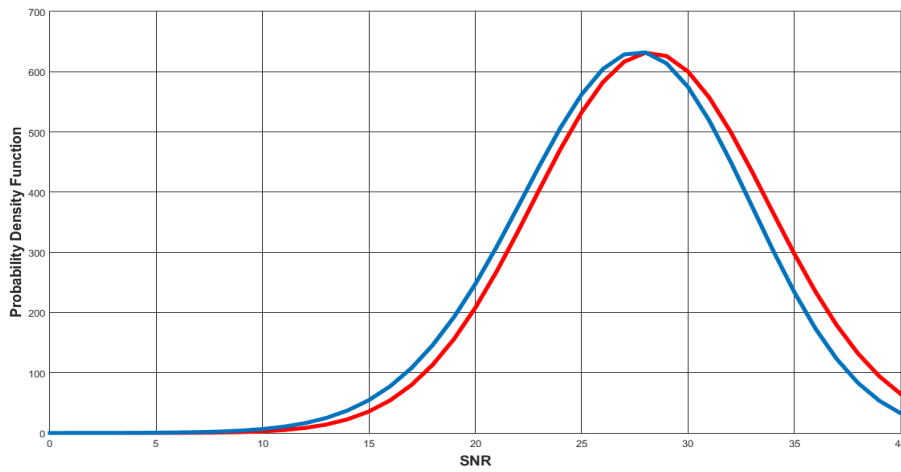


Figure 30 Comparisons of Results for $\bar{\mu} = 25$

For $\bar{\mu} = 30$, coefficients of polynomial equations are given in (3.47). Graphs of A , B and C coefficients with respect to length are depicted in Fig. 33, 34 and 35. We plot the pdf obtained using the numerical integration and the one obtained using the modeling technique presented in this thesis work for $\bar{\mu} = 30$ in Fig.36.

$$p1X^6 + p2X^5 + p3X^4 + p4X^3 + p5X^2 + p6X^1 + p7.$$

A ▶	P1	P2	P3	P4	P5	P6	P7	
	-0.8659	-21.56	80.18	89.19	-410.4	1103	3078	
B ▶	P1	P2	P3	P4	P5	P6	P7	
	0.01401	-0.023	-0.056	0.1009	-0.3466	-1.52	31.24	
C ▶	P1	P2	P3	P4	P5	P6	P7	
	0.00560	-0.018	-0.039	0.1423	0.2551	4.585	11.43	(3.47)

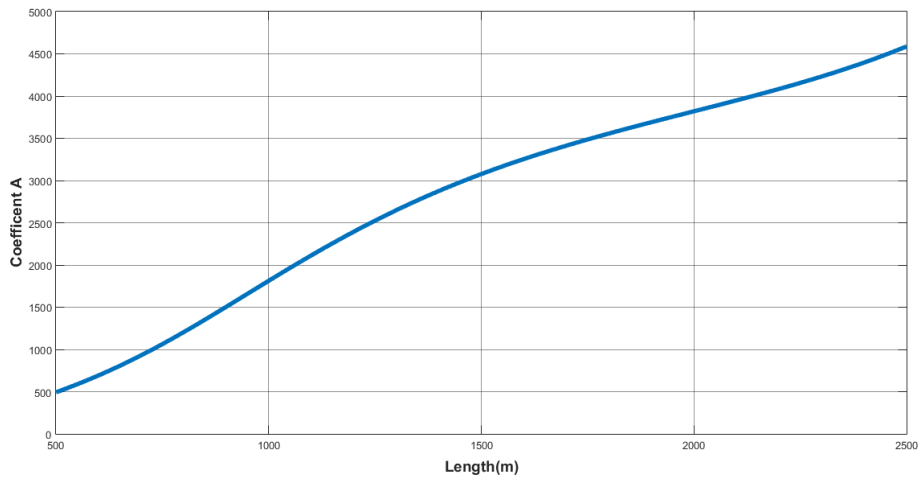


Figure 31 Change of A with respect to L for $\bar{\mu} = 30$

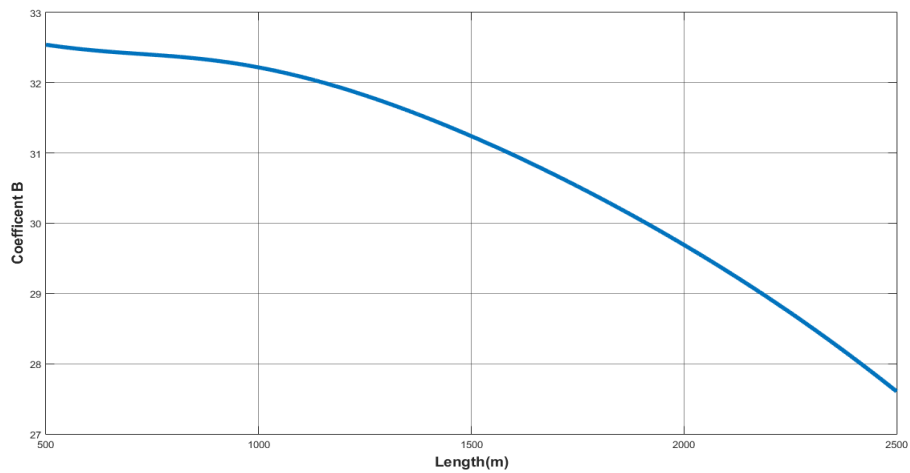


Figure 32 Change of B with respect to L for $\bar{\mu} = 30$

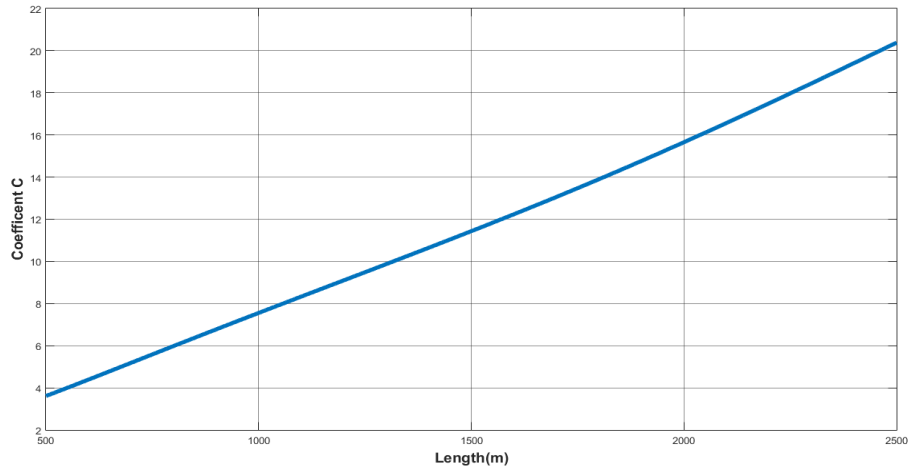


Figure 33 Change of C with respect to L for $\bar{\mu} = 30$

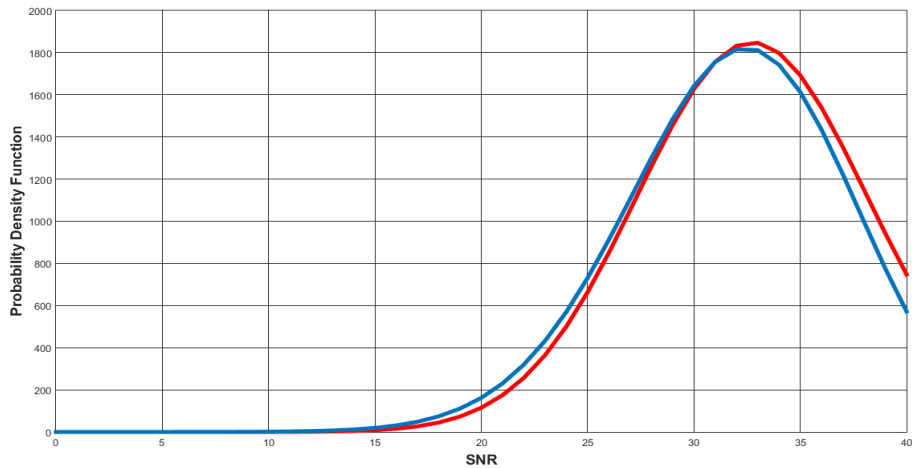


Figure 34 Comparisons of Results for $\bar{\mu} = 30$

For $\bar{\mu} = 35$, coefficients of polynomial equations are given in (3.48). Graphs of A , B and C coefficients with respect to length are depicted in Fig. 37, 38 and 39. We plot the pdf obtained using the numerical integration and the one obtained using the modeling technique presented in this thesis work for $\bar{\mu} = 35$ in Fig.40.

$$p1X^6 + p2X^5 + p3X^4 + p4X^3 + p5X^2 + p6X^1 + p7.$$

A ▶	P1	P2	P3	P4	P5	P6	P7	
	25.87	-25.26	-110	342.9	-318.1	549.9	5111	
B ▶	P1	P2	P3	P4	P5	P6	P7	
	0.0021	0.0026	-0.050	0.0310	-0.1771	-2.129	34.98	
C ▶	P1	P2	P3	P4	P5	P6	P7	
	-0.0022	-0.011	-0.010	0.1516	0.2688	4.36	11.14	(3.48)

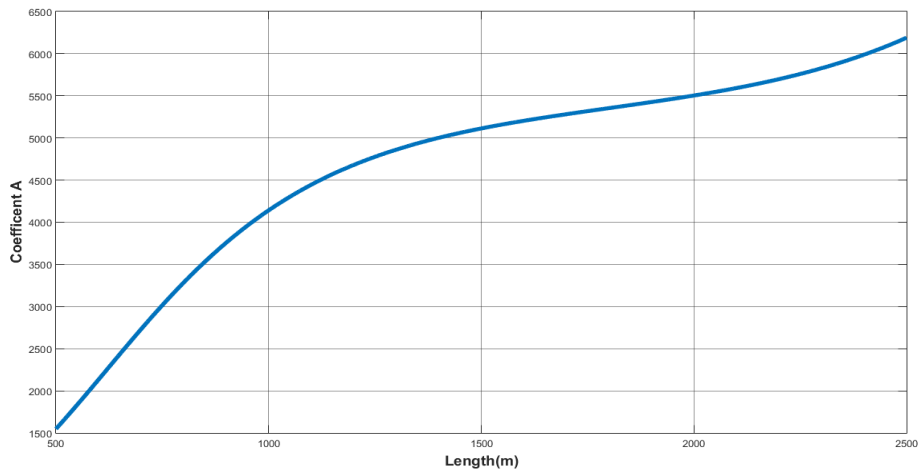


Figure 35 Change of A with respect to L for $\bar{\mu} = 35$

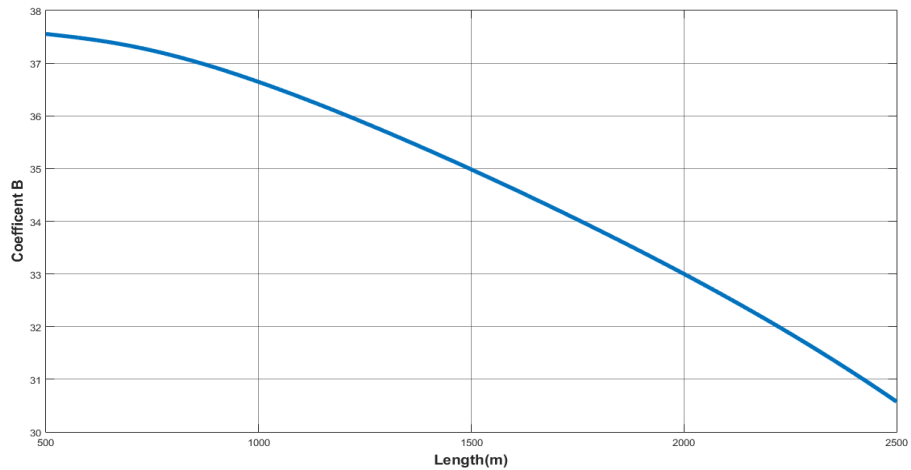


Figure 36 Change of B with respect to L for $\bar{\mu} = 35$

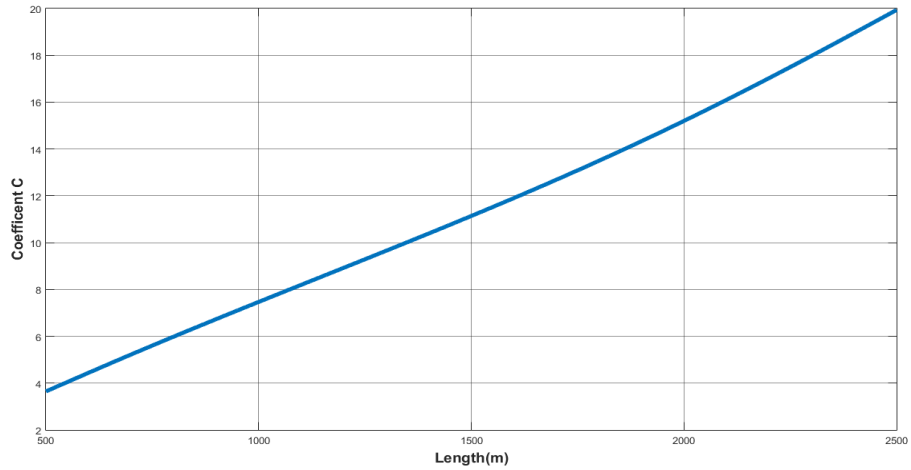


Figure 37 Change of C with respect to L for $\bar{\mu} = 35$

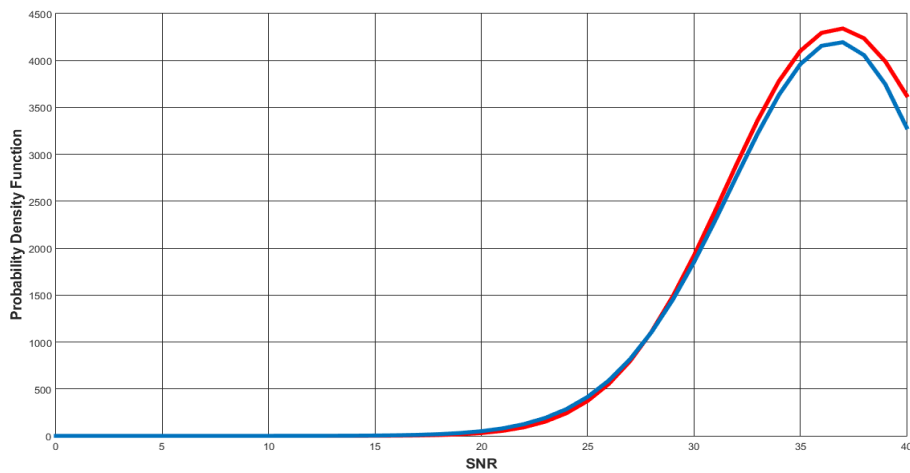


Figure 38 Comparisons of Results for $\bar{\mu} = 35$

For $\bar{\mu} = 40$, coefficients of polynomial equations are given in (3.49). Graphs of A , B and C coefficients with respect to length are depicted in Fig. 41, 42 and 43. We plot the pdf obtained using the numerical integration and the one obtained using the modeling technique presented in this thesis work for $\bar{\mu} = 40$ in Fig.44.

$$p1X^6 + p2X^5 + p3X^4 + p4X^3 + p5X^2 + p6X^1 + p7.$$

A ▶	P1	P2	P3	P4	P5	P6	P7	
	-16.04	50.97	-19.14	88.65	53.49	144.3	6533	
B ▶	P1	P2	P3	P4	P5	P6	P7	
	-0.0075	0.0097	-0.005	-0.040	-0.030	-2.71	38.42	
C ▶	P1	P2	P3	P4	P5	P6	P7	
	-0.005	-0.0063	0.010	0.146	0.2789	4.122	10.89	(3.49)

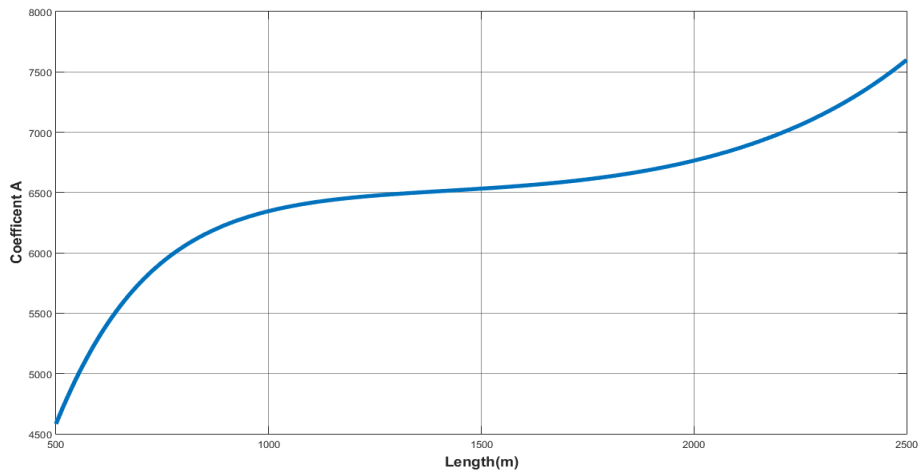


Figure 39 Change of A with respect to L for $\bar{\mu} = 40$

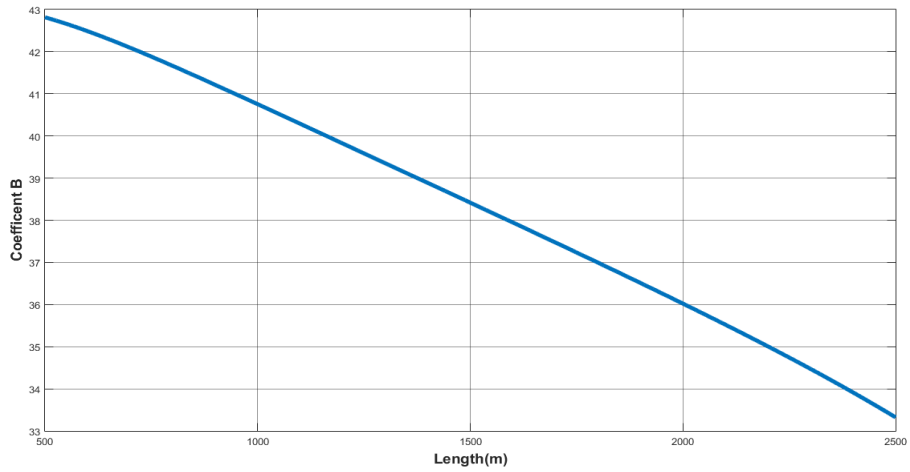


Figure 40 Change of B with respect to L for $\bar{\mu} = 40$

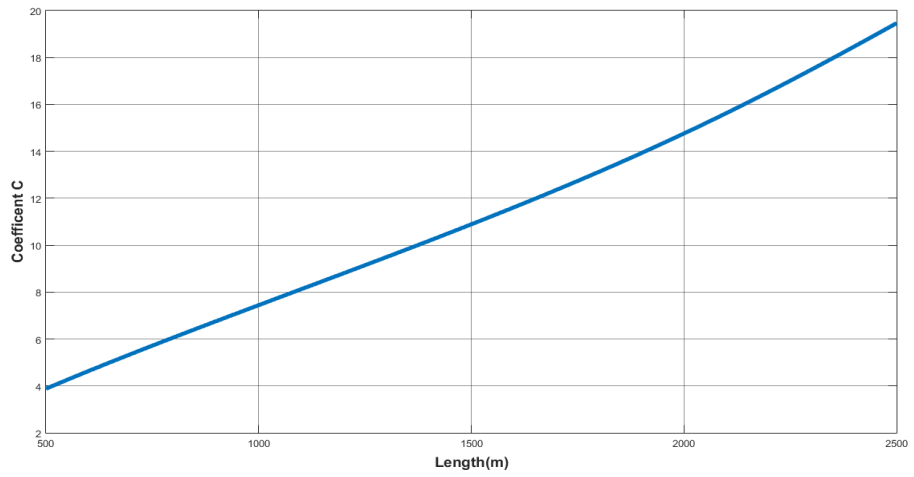


Figure 41 Change of C with respect to L for $\bar{\mu} = 40$

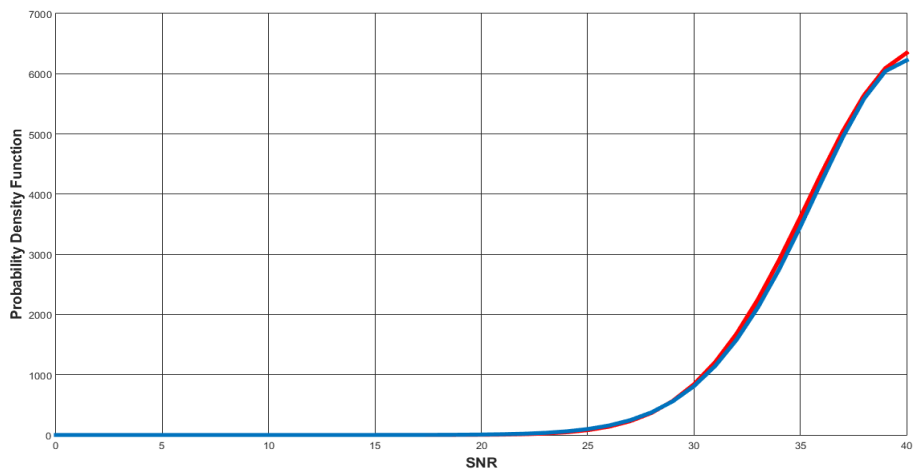


Figure 42 Comparisons of Results for $\bar{\mu} = 40$

3.7 Average Probability of Transmission Error Rate

In this section, we calculate A, B and C coefficient values for 8 $\bar{\mu}$ values ranging from 0 to 40. For the calculation of coefficient values we use MATLAB curve fitting option for $p(x)$ equation which is defined in expression (2.16). Coefficient values are tabulated in Fig. 45.

$\bar{\mu}$	A	B	C
$\bar{\mu} = 5$	10,96	7,835	9,283
$\bar{\mu} = 10$	33,64	12,76	9,425
$\bar{\mu} = 15$	105,7	17,73	9,46
$\bar{\mu} = 20$	326,9	22,66	9,414
$\bar{\mu} = 25$	951,2	27,44	9,284
$\bar{\mu} = 30$	2393	31,92	9,098
$\bar{\mu} = 35$	4680	36,03	8,925
$\bar{\mu} = 40$	6459	39,82	8,803

Table 3 List of Coefficients for Different $\bar{\mu}$ Values

After calculation of coefficient values, we compute probability of average transmission error with respect to average signal to noise ratio (SNR). We use the equation in (3.50) to calculate P_e values

$$P_e = \left(\frac{1}{\pi} \int_0^{\frac{\pi}{2}} M_s \left(\frac{\Psi}{\sin^2 \theta} \right) d\theta \right). \quad (3.50)$$

In (3.50) M_s represents the moment generating function defined in (3.8). We assign $\sin^2 \theta = S$, $\Psi = 1/2$. After these assignments equation (3.50) becomes as in (3.51).

$$P_e = \left(\frac{1}{\pi} \int_0^{\frac{\pi}{2}} M_s \left(\frac{1}{2S} \right) dS \right) \quad (3.51)$$

We calculate all P_e values with respect to SNR ranging from 0 to 40 in steps of 5. We plot transmission error probability P_e with respect to Signal to noise ratio (SNR) in Fig. 45.

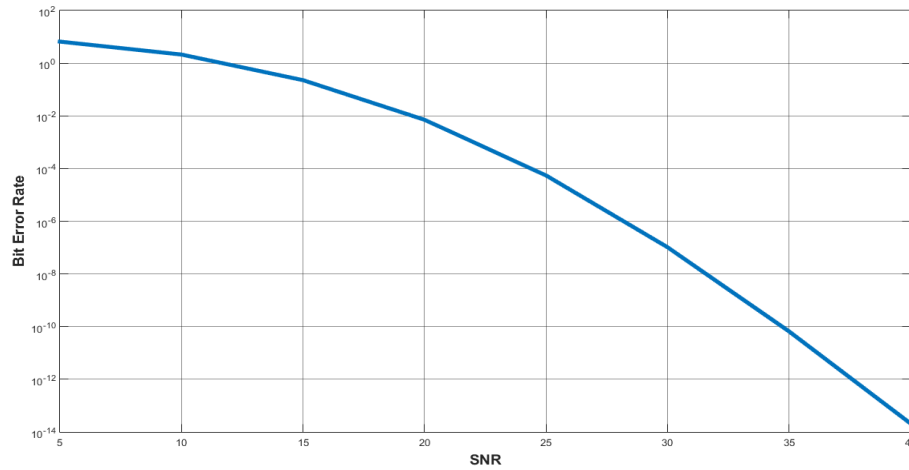


Figure 43 Average Probability of Transmission Error Rate to SNR

From this Fig. 45, it is obvious that as the average SNR increases, probability of transmission error decreases rapidly. Thus for $\bar{\mu} = 40$ dB the probability of transmission error is less than 10^{-12}

CHAPTER 4

CONCLUSION

In this thesis study, we demonstrated how to develop a mathematical model in closed form for those systems having performance expressions in numerical integration form. For this purpose, we considered two-hop communication systems whose end-to-end performance depends on the harmonic mean of the hop SNRs. We considered two-hop systems with log-normally distributed optical communication channels. We derived an expression for the harmonic mean of two-hop systems employing log-normally distributed channels. Later, for the derived expression, using the curve fitting utility of the MATLAB compiler, we developed a simple Gaussian like expression for the derived harmonic mean expression, and using the developed approximate expression we calculated the cumulative distribution function, moment generating function, and transmission error probability, for two-hop communication systems with log-normal channels.

FSO offers many advantages over existing techniques which can be either optical or radio or microwave. Less cost and time to setup are the main attraction of FSO system. Optical equipment can be used in FSO system with some modification. Merits of FSO communication system and its application area make it a hot technology but there are some problems arising due to the attenuation caused by medium. FSO system poses some problem like attenuation in medium that can affect the performance of transmission as power loss would be there. But extra care and restudy of the medium can guide what type of parameters to be considered before setting up the system.

In this work, we have derived closed-form expression for the evaluation of the average capacity and the outage probability of a typical two-hop FSO

communication system over turbulence atmospheric conditions modeled by log normal distribution respectively. We studied the dependence of the reliability and the performance of a system as a function of the principal parameters of such a link, being the length of the link, aperture diameter of the receiver and the atmospheric turbulence conditions between transmitter and receiver. If we know the value of length between transmitter and receiver and turbulence strength according to atmospheric conditions, we can calculate performance of channels easily thanks to our model which is explained in this thesis.



REFERENCES

1. **Mazen O. Hasna, Mohamed-Slim Alouini**, “*Harmonic Mean and End-To-End Performance of Transmission Systems with Relays*”. IEEE Trans. on Commun. vol. 52, No1, January 2004.
2. **Shlomi Arnon, David M. Britz, Anthony C. Boucouvalas, and Mohsen Kavehrad**, “*Optical wireless communications: introduction to the feature issue*,” J. Opt. Netw. 5, 79-81 (2006).
3. **A. K. Majumdar**, “*Free-Space Laser Communication Performance in the Atmospheric Channel*,” J. Opt. Fiber. Commun. Rep. 2(4), 345–396 (2005).
4. **<http://www.fsona.com/solutions.php>** “*Optical wireless communication solutions*” (Data download date 01.08.2017).
5. **P.Schoon**, “*Free Space Optics in the Enterprise Market*,” System Support Solutions Inc., February 2003.
6. **M. D. Springer**, “*The algebra of random variables*”. New York: Wiley, 1979.
7. **Gradshteyn, I. S., and Ryzhik, I. W.**, “*Table of Integrals, Series and Products*”. 5th ed. San Diego, CA: Academic (Academic Press, 1994).
8. **M. Abramowitz and I.A. Stegun** , “*Handbook of Mathematical Functions With Formulas, Graphs, and Mathematical Tables*” 9th. Ed. New York: Dover, 1970

9. **Andrews L.C., AL-Habash M.A., Hopen C.Y., Phillips R.L.**, “*Theory of Optical Scintillation: Gaussian Beam Wave Model*” *Waves Random Med.*, 2001, 11, pp. 271-279.
10. **M. K. Simon and M.-S Alouini**, “*Digital Communication over Fading Channels*”. New York: Wiley 1988.
11. **H. E. Nistazakis, T.A Tsiftsis, G.S. Tombras**, “*Performance Analysis of Free-Space Optical Communication Systems Over Atmospheric Turbulence Channels*” Published in *IET Communications* 18th November 2008 doi:10.1049/iet.com.2008.0
12. **A. Papoulis**, “*Probability Random Variables and Stochastic Processes*” 3rd Ed. New York: McGraw-Hill, 1991.
13. **A. Sendonaris, E. Erkip, and B. Aazhang**, “*Increasing Uplink Capacity via user cooperation diversity*” in *Proc. IEEE Int. Symp. Information Theory (ISIT’98)*, Cambridge, MA, Aug. 1998, p.156.
14. **R. M. Gagliardi**, “*Introduction to Engineering*”, New York: Wiley 1988.
15. **A. Erdelyi, W. Magnus, F. Oberhettinger, and F. Tricomi**. “*Table of Integral Transforms.*” New York: McGraw-Hill, 1954, vol. 2.
16. **M. Nakagami**. “*The m-distribution-a general formula of intensity distribution of rapid fading*”, in *Statistical Methods in Radio Wave Propagation.*” Oxford, U.K. : Pergamon, 1960, pp.3-36.
17. **H. G. Sandalidis, T. A. Tsiftsis, G. K. Karagiannidis, M. Uysal**. “*BER Performance of FSO Links over Atmospheric Turbulence Channels with Pointing Errors.*” *IEEE Commun Lett.*, 2008, 12, (1), pp.44-46.

18. **D. Kedar, S. Arnon.** “*Urban Optical Wireless Communication Network: The Main Challenges and Possible Solutions*” IEEE Optical Communications Supplement to IEEE Communications Magazine, 2004, pp. S1-S7.

19. **H. G. Sandalidis, T. A. Tsiftsis.** “*Outage Probability and Ergodic Capacity of Free Space Optical Links Over Strong Turbulence.*” Electron. Lett., 2008, 44, (1), pp. 46-47.

20. **T.A. Tsiftsis.** “*Performance of Heterodyne Wireless Optical Communications Systems over Gamma-Gamma Atmospheric Turbulence Channels.*” Electron. Lett. 2008, 44,(5), pp. 373-375.

APPENDICES A
CURRICULUM VITAE

PERSONAL INFORMATION

Surname, Name: Görse, Serkan

Date and Place of Birth: 20 February 1989, Ankara

Marital Status: Single

Phone: +90 538 545 5320

Email: gorse.serkan@gmail.com

EDUCATION

Degree	Institution	Year of Graduation
B.Sc.	Cankaya Univ., Electronic and Communication Engineering	2012
High School	Inonu High School	2006

WORK EXPERIENCE

Year	Place	Enrollment
2016-Present	THALES	High Speed Trains Signalization System Chief Engineer
2015-2016	Proland Group	Medical Devices Supervisor
2013 - 2015	GATE Electronic Inc.	R&D Engineer

FOREIN LANGUAGES

English

PROJECTS

**May 2016 –
Present**

Company: THALES

Department: Technical Department of Maintenance

Project Definition: My responsibilities are stated below in this position;

1-Communicating with TCDD site staff about maintenance problems regularly for progress payment.

2-Fulfillment of the duties of maintenance department

3-Control of version, application and updates

4-Monitoring and control of the situation and reporting

5-Preventive Maintenance Activity

6-Troubleshooting and Corrective Maintenance Activity

7-Reporting failure statistics monthly and yearly.

**April 2016 –
May 2016**

Company: Altay Kollektif

Department: MGEO Aselsan Team

Project Definition: Producing embedded test software for unmanned aerial vehicle which name is ANKA. In this project I am producing some embedded software in C++ for making functionality tests of ANKA.

**October 2015 -
April 2016**

Company: Proland Group

Department: Medical Devices Department

Project Definition: I was designing embedded software for medical devices and I was coordinating production of these devices for all hospitals in Turkey.

**August 2014 -
February 2015**

Company: GATE Electronic Inc.

Department: Communication-Electronics Systems Team

Project Name: PXI – DAQ Data Acquisition Card

Project Definition: I was designing embedded software for an FPGA module and PCB. While I was designing PCB card and embedded software I used Altium Designer and MPLAB packet programs.

**August 2014 -
October 2015**

Company: GATE Electronic Inc.

Department: Communication-Electronics Systems Team

Project Name: DSBCA

Project Definition: In this project I produce a program for testing electronic card which are using in Cougar Helicopters using by Turkish air forces.

**April 2013 -
November 2014**

Company: GATE Electronic Inc.

Department: Communication-Electronics Systems Team

Project Name: Portable Jammer Tester

Project Definition: In this project I produce an embedded program and a PCB card for testing Jammers which are using in Turkish army. Thanks to this device soldiers can test their jammers while they are on the area

**April 2013 -
August 2014**

Company: GATE Electronic Inc.

Department: Communication-Electronics Systems Team

Project Name: GATESEM

Project Definition: In this project I produce an embedded program which is integrated with walkie-talkie using by police forces. Thanks to this program police forces communicate with an encryption algorithm.

HOBBIES

Travelling, Football, Basketball, Cinema